

# Scaffold Functions of 14-3-3 Adaptors in B Cell Immunoglobulin Class Switch DNA Recombination

Tonika Lam<sup>1,2,3</sup>, Lisa M. Thomas<sup>1,3,4</sup>, Clayton A. White<sup>1</sup>, Guideng Li<sup>1</sup>, Egest J. Pone<sup>1</sup>, Zhenming Xu<sup>1,2</sup>, Paolo Casali<sup>1,2\*</sup>

**1** Institute for Immunology, School of Medicine and School of Biological Sciences, University of California Irvine, Irvine, California, United States of America, **2** Department of Microbiology and Immunology, School of Medicine, University of Texas Health Science Center at San Antonio, San Antonio, Texas, United States of America

## Abstract

Class switch DNA recombination (CSR) of the immunoglobulin heavy chain (*IgH*) locus crucially diversifies antibody biological effector functions. CSR involves the induction of activation-induced cytidine deaminase (AID) expression and AID targeting to switch (S) regions by 14-3-3 adaptors. 14-3-3 adaptors specifically bind to 5'-AGCT-3' repeats, which make up for the core of all *IgH* locus S regions. They selectively target the upstream and downstream S regions that are set to undergo S-S DNA recombination. We hypothesized that 14-3-3 adaptors function as scaffolds to stabilize CSR enzymatic elements on S regions. Here we demonstrate that all seven 14-3-3 $\beta$ , 14-3-3 $\epsilon$ , 14-3-3 $\gamma$ , 14-3-3 $\eta$ , 14-3-3 $\sigma$ , 14-3-3 $\tau$  and 14-3-3 $\zeta$  adaptors directly interacted with AID, PKA-C $\alpha$  (catalytic subunit) and PKA-Rl $\alpha$  (regulatory inhibitory subunit) and uracil DNA glycosylase (Ung). 14-3-3 adaptors, however, did not interact with AID C-terminal truncation mutant AID $\Delta$ (180–198) or AIDF193A and AIDL196A point-mutants (which have been shown not to bind to S region DNA and fail to mediate CSR). 14-3-3 adaptors colocalized with AID and replication protein A (RPA) in B cells undergoing CSR. 14-3-3 and AID binding to S region DNA was disrupted by viral protein R (Vpr), an accessory protein of human immunodeficiency virus type-1 (HIV-1), which inhibited CSR without altering AID expression or germline I<sub>H</sub>-C<sub>H</sub> transcription. Accordingly, we demonstrated that 14-3-3 directly interact with Vpr, which in turn, also interact with AID, PKA-C $\alpha$  and Ung. Altogether, our findings suggest that 14-3-3 adaptors play important scaffold functions and nucleate the assembly of multiple CSR factors on S regions. They also show that such assembly can be disrupted by a viral protein, thereby allowing us to hypothesize that small molecule compounds that specifically block 14-3-3 interactions with AID, PKA and/or Ung can be used to inhibit unwanted CSR.

**Citation:** Lam T, Thomas LM, White CA, Li G, Pone EJ, et al. (2013) Scaffold Functions of 14-3-3 Adaptors in B Cell Immunoglobulin Class Switch DNA Recombination. PLoS ONE 8(11): e80414. doi:10.1371/journal.pone.0080414

**Editor:** Kefei Yu, Michigan State University, United States of America

**Received:** April 19, 2013; **Accepted:** October 2, 2013; **Published:** November 25, 2013

**Copyright:** © 2013 Lam et al. This is an open-access article distributed under the terms of the Creative Commons Attribution License, which permits unrestricted use, distribution, and reproduction in any medium, provided the original author and source are credited.

**Funding:** This work was supported by United States National Institutes of Health grants AI 079705, AI 10105813 and AI 060573 (to P.C.), and T. Lam is supported by the AI 060573 T32 training grant. The funders had no role in study design, data collection and analysis, decision to publish, or preparation of the manuscript.

**Competing Interests:** The authors have declared that no competing interests exist. Lisa M. Thomas performed experiments at the University of California, Irvine, prior to her employment at the Novartis Institute (San Diego, California, United States of America).

\* E-mail: pcasali@uci.edu

‡ Current address: Genomic Institute of the Novartis Research Foundation, San Diego, California, United States of America

§ These authors contributed equally to this work.

## Introduction

Immunoglobulin (Ig) class switch DNA recombination (CSR) and somatic hypermutation (SHM) are central to the maturation of the antibody response for the effectiveness of vaccines and the generation of neutralizing antibodies to microbial pathogens (including bacteria and viruses) and tumoral cells as well as the maturation of the autoantibody response in systemic or organ-specific autoimmunity. CSR irreversibly substitutes the Ig heavy chain (*IgH*) constant (C<sub>H</sub>) region, for instance, C $\mu$  for IgM – which is expressed in all naïve B cells – with a downstream C<sub>H</sub> region, C $\gamma$ , C $\epsilon$  or C $\alpha$  [1,2], thereby giving rise to IgG, IgE or IgA antibodies without altering the structure of the antigen-binding site [3,4]. Class-switched IgG, IgE and IgA antibodies display different tissue distributions and possess diverse biological effector functions. SHM inserts mainly single nucleotide point-mutations into the antibody recombined V(D)J segments at a high rate to provide the structural substrate for positive selection of high affinity mutants by foreign antigen [5,6].

CSR (as well as SHM) occur in B lymphocytes activated in peripheral lymphoid organs. CSR critically requires germline I<sub>H</sub>-C<sub>H</sub> transcription of the upstream, e.g., I $\mu$ , and downstream I $\gamma$ , I $\epsilon$  or I $\alpha$  subloci [4]. Germline I<sub>H</sub>-C<sub>H</sub> transcription initiates at the intervening I $\mu$ , I $\gamma$ , I $\epsilon$  or I $\alpha$  promoter and elongates through the I<sub>H</sub> exon, intronic switch (S) region, and the C<sub>H</sub> exon cluster, giving rise to germline I $\mu$ -C $\mu$ , I $\gamma$ -C $\gamma$ , I $\alpha$ -C $\alpha$  or I $\epsilon$ -C $\epsilon$  transcripts. CSR also requires activation-induced cytidine deaminase (AID, encoded by *AICDA* in humans and *Aicda* in mice), which is expressed at high levels in activated B lymphocytes, including those in germinal centers [7–9]. AID is a member of the AID/APOBEC cytidine deaminase family; it deaminates deoxycytosines (dCs) in S region DNA, yielding deoxyuracils (dUs) [10,11]. The processing of dUs by uracil DNA glycosylase (Ung) results in abasic sites, nicking of which by apurinic/apyrimidic endonucleases (APEs) leads to generation of DNA double-strand breaks (DSBs) in the upstream (donor, e.g., S $\mu$ ) and downstream (acceptor) S regions that are obligatory intermediates of CSR [12]. CSR then proceeds through DSB resolution [13]; synapsis of

the upstream and downstream DSBs occurs through excision of the intervening DNA from the chromosome to form a switch DNA circle and leads to S-S DNA junctions. Switch DNA circles are transiently transcribed, giving rise to circle  $I\gamma$ -C $\mu$ ,  $I\epsilon$ -C $\mu$  or  $I\alpha$ -C $\mu$  transcripts, which are hallmarks of ongoing CSR [14]. Post-recombined *IgH* DNA sequences are transcribed, giving rise to post-recombination  $I\mu$ -C $\gamma$ ,  $I\mu$ -C $\epsilon$  or  $I\mu$ -C $\alpha$  transcripts, and mature  $V_HDJ_H$ -C $\gamma$ ,  $V_HDJ_H$ -C $\epsilon$  or  $V_HDJ_H$ -C $\alpha$  transcripts, which encode IgG, IgE or IgA, respectively [4].

Triggering of CSR requires both “primary” and “secondary” CSR-inducing stimuli [4]. Primary CSR-inducing stimuli

comprise a T-dependent stimulus, i.e., engagement of CD40 expressed on B cells by trimeric CD154 expressed on CD4<sup>+</sup> T cells, or a T-independent stimuli, such as dual engagement of Toll-like receptors (TLRs) and B cell receptor (BCR). Such dual engagement is exemplified by *E. coli* lipopolysaccharides (LPS), which engages TLR4 and BCR through its monophosphoryl lipid A and polysaccharide moieties, respectively [4,15,16]. Secondary CSR-inducing stimuli consist of cytokines such as interleukin-4 (IL-4), transforming growth factor- $\beta$  (TGF- $\beta$ ) and interferon- $\gamma$  (IFN- $\gamma$ ), which selectively and specifically induce germline  $I\gamma$ -C $\gamma$  and  $I\epsilon$ -C $\epsilon$  (IL-4) or  $I\gamma$ 2b-C $\gamma$ 2b and  $I\alpha$ -C $\alpha$  (TGF- $\beta$ ) or  $I\gamma$ 2a-C $\gamma$ 2a

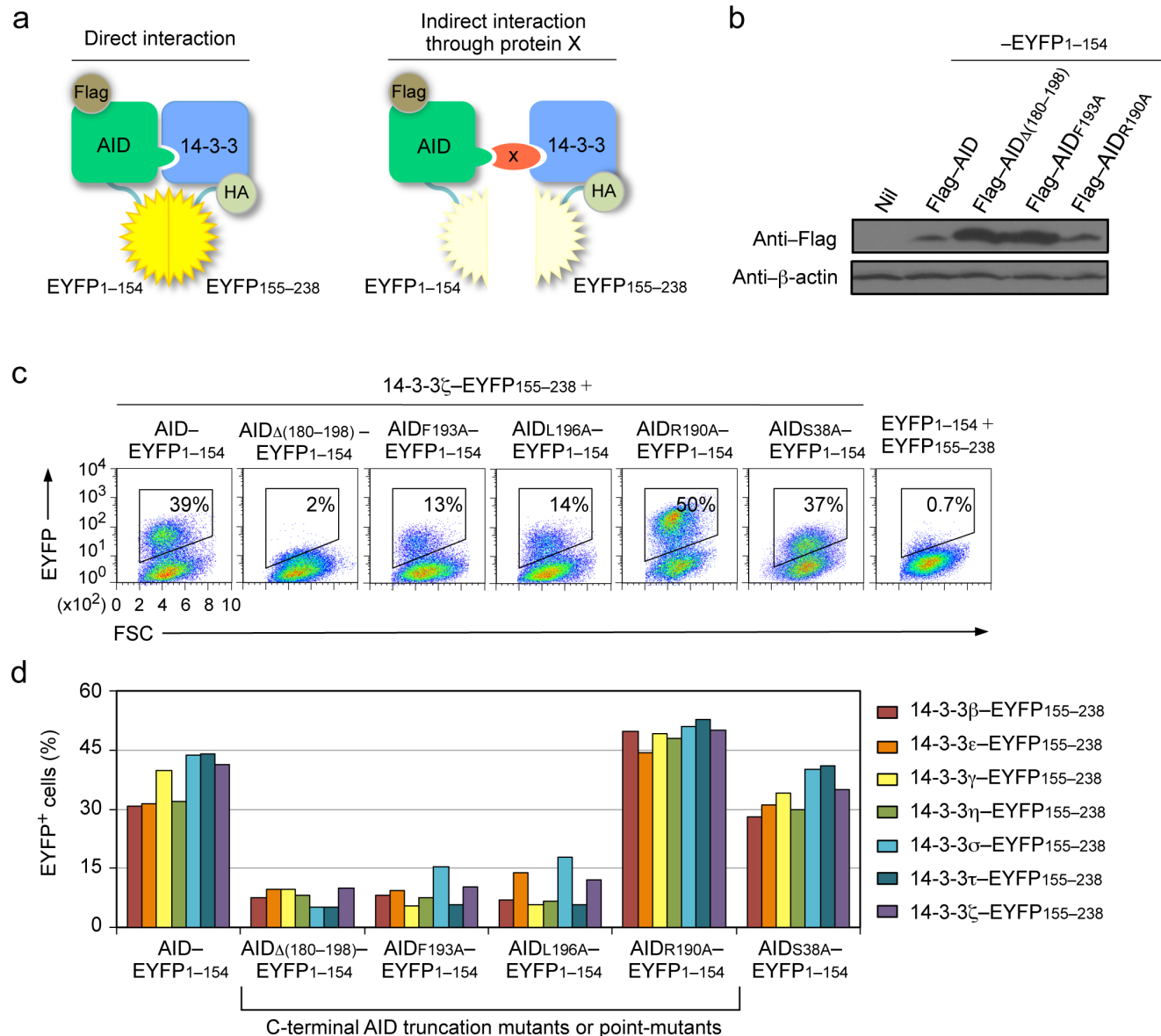


**Figure 1. 14-3-3 adaptors interact with AID through the AID C-terminus.** (a) Schematics of the principle of the BiFC assays to analyze interaction of 14-3-3 (HA-14-3-3-EYFP155-238) and AID (Flag-AID-EYFP1-154). (b) Immunoblotting using specific mAbs to identify Flag and  $\beta$ -actin in HeLa cell expressing nil (pcDNA3 vector), Flag-AID, Flag-AID $\Delta$ (180-198), Flag-AIDF193A, Flag-AIDR190A (fused to EYFP1-154). (c) BiFC assays of the interaction between 14-3-3 $\zeta$  (fused to EYFP155-238) and AID, and AIDR190A and AIDS38A, but not AID $\Delta$ (180-198), AIDF193A or AIDL196A (fused to EYFP1-154) in HeLa cells (at 24 hours), as analyzed by flow cytometry. (d) Quantification of the interaction between each of the seven 14-3-3 isoforms ( $\beta$ ,  $\epsilon$ ,  $\gamma$ ,  $\eta$ ,  $\sigma$ ,  $\tau$ ,  $\zeta$ ; fused to EYFP155-238) and AID, AID $\Delta$ (180-198), AIDF193A, AIDL196A, AIDR190A or AIDS38A (fused to EYFP1-154), in HeLa cells (at 48 hours) depicted as percentage of EYFP<sup>+</sup>, as analyzed by flow cytometry. Data are representative of those from three independent experiments.

doi:10.1371/journal.pone.0080414.g001

(IFN- $\gamma$ , in mouse but not human) transcription. Primary stimuli induce B cells to proliferate and express AID and other CSR-related genes. They also enable secondary stimuli to direct CSR to specific immunoglobulin isotypes [17,18].

For CSR to unfold, AID and the whole CSR machinery must be targeted to the S regions that are set to undergo recombination to introduce DSBs, the resolution of which leads to S-S DNA recombination – dysregulation of AID expression and targeting has been associated with chromosomal translocations, lymphomagenesis and autoimmunity [19–22]. In species that use CSR to diversify their antibodies, all S region “cores”, within which DSBs and S-S junctions preferentially segregate, contain high-density repeats of the 5'-AGCT-3' motif [23,24]. 14-3-3 adaptor proteins (seven homologous isoforms, 14-3-3 $\beta$ , 14-3-3 $\epsilon$ , 14-3-3 $\gamma$ , 14-3-3 $\eta$ , 14-3-3 $\sigma$ , 14-3-3 $\tau$  and 14-3-3 $\zeta$ ) [25,26] specifically bind to 5'-AGCT-3' repeats and are selectively recruited to the upstream and downstream S regions that are set to undergo S-S DNA recombination by the H3K9acS10ph combinatorial histone modification [17,23]. Once docked onto S regions, 14-3-3 adaptors mediate the assembly of macromolecular complexes on S region DNA. This notion is indeed supported by our demonstration that 14-3-3 adaptors recruit/stabilize AID and protein kinase A (PKA), which phosphorylates AID at serine (Ser)38, on S regions [23,27,28] and that that all seven 14-3-3 isoforms directly interact with AID and PKA catalytic subunit (PKA-C $\alpha$ ) and that 14-3-3 $\gamma$ , 14-3-3 $\sigma$  and 14-3-3 $\zeta$  enhance AID dC DNA deamination activity [23].

Here, we hypothesized that 14-3-3 adaptors function as structural scaffolds to stabilize multiple enzymatic elements on S regions in CSR. To test our hypothesis, we adapted the bimolecular fluorescence complementation (BiFC) assay to quantify the direct interaction between all seven isoforms of 14-3-3 adaptors with CSR factors, such as AID, PKA, RPA, Ung, or with AID mutants or Ung mutants that cannot mediate CSR. We also used (GST) pull-down assay to show that 14-3-3 interact with AID, PKA and Ung. Finally, we quantified the direct interaction between 14-3-3, AID, PKA or Ung and viral protein R (Vpr), an accessory protein of the human immunodeficiency virus type-1 (HIV-1) and utilized this naturally occurring viral protein to disrupt 14-3-3 and AID binding to S region DNA, which inhibited CSR. Thus, our findings suggest that 14-3-3 adaptors play important scaffold functions and nucleate the assembly of multiple CSR factors on S regions and that small molecule compounds that specifically disrupt their interactions can be used to inhibit unwanted CSR, such as CSR underlying the generation of IgG and IgA autoantibodies in autoimmunity and atopic IgE antibodies in allergies and asthma.

## Materials and Methods

### B Lymphocytes

Spontaneously switching human sIg $\mu^+$  sIg $\delta^+$ 4B6 B cells and inducible switching human sIg $\mu^+$  sIg $\delta^+$ 2E2 B cells were derived from the CSR- and SHM-inducible human monoclonal sIg $\mu^+$  sIg $\delta^+$  CL-01 B cell line [23,29,30]. Single B cell suspensions were prepared from murine spleens using a 70  $\mu$ m cell strainer. B cells were suspended in RPMI-1640 medium (Invitrogen) supplemented with FBS (10% v/v, Thermo Scientific), penicillin-streptomycin and amphotericin B fungizone (1% v/v) and 50  $\mu$ M  $\beta$ -mercaptoethanol (FBS-RPMI) [16].

### Class Switch DNA Recombination

To analyze CSR by surface Ig, sIg $\mu^+$  sIg $\delta^+$  murine B cells were cultured at  $10^5$  cell/ml in FBS-RPMI in the presence of LPS

deproteinized by chloroform extraction (3  $\mu$ g/ml, from *E. coli*, serotype 055:B5, Sigma-Aldrich) plus recombinant mIL-4 (4 ng/ml, R&D Systems) for CSR from IgM to IgG1. B cells were harvested and stained using phycoerythrin (PE)-labeled anti-mouse B220 mAb (clone RA3-6B2, BD Biosciences), 7-aminocoumarin D (7-AAD, Sigma-Aldrich) and allophycocyanin (APC)-labeled anti-mouse IgG1 mAb (clone X56, BD Biosciences) using FACSCalibur<sup>TM</sup> flow cytometer (BD Biosciences). Dead (7-AAD<sup>+</sup>) cells were excluded from analysis.

### Bimolecular Fluorescence Complementation (BiFC)

BiFC assays were performed as we described [23]. Briefly, EYFP was split into two complementary moieties: the N-terminal 154 amino acids (EYFP1–154) and the C-terminal 84 amino acids (EYFP155–238). EYFP1–154 was fused with Flag-tagged AID or AID mutants, PKA-C $\alpha$ , PKA-R1 $\alpha$ , RPA1, Ung or Ung mutants, or 14-3-3 $\zeta$ ; EYFP155–238 was fused with influenza hemagglutinin (HA)-tagged 14-3-3 $\beta$ ,  $\epsilon$ ,  $\gamma$ ,  $\eta$ ,  $\sigma$ ,  $\tau$  or  $\zeta$ , or Vpr.  $5 \times 10^5$  HeLa cells cultured in DMEM (Invitrogen) supplemented with FBS, were transfected with 1  $\mu$ g of plasmid using Lipofectamine<sup>TM</sup> (Life Technologies). After 24 hours, cells were analyzed for cell viability (7-AAD<sup>+</sup>) and for EYFP intensity by FACSCalibur<sup>TM</sup> flow cytometer (BD Biosciences); after 36 hours, cells were imaged for cell viability (ProLong Gold Antifade Reagent with 4',6'-diamidino-2-phenylindole, DAPI, Invitrogen) and for EYFP intensity by an Olympus FluoView 1000 confocal microscope.

### Chromatin Immunoprecipitation (ChIP)

ChIP assays were performed as we described [23]. B cells were treated with 1% (v/v) formaldehyde for 10 min at 25°C to crosslink chromatin before being washed with cold PBS containing protease inhibitors (Roche) and resuspended in lysis buffer (20 mM Tris-HCl, 200 mM NaCl, 2 mM EDTA, 0.1% w/v SDS and protease inhibitors, pH 8.0). Chromatin was sonicated to yield DNA fragments (about 200 to 600 bps), pre-cleared with protein A agarose beads (Pierce) and then incubated with rabbit anti-14-3-3 $\gamma$  Ab (catalog # 18647, IBL, Inc.) or mouse anti-AID mAb (catalog # 39-2500, Invitrogen) overnight at 4°C. Immune complexes were precipitated by Protein A agarose beads, washed and then eluted with elution buffer (50 mM Tris-HCl, 0.5% SDS, 200 mM NaCl, 100  $\mu$ g/ml proteinase K, pH 8.0), followed by incubation at 65°C for 4 hours to reverse formaldehyde cross-links and digest proteins. DNA in the supernatant was purified using a QIAquick PCR purification kit (Qiagen). Recovered DNA was specified by PCR using the following oligonucleotide primers: S $\mu$ , forward 5'-GCTAAACTGAGGTGATTACTCTGAGGTAAG-3' and reverse 5'-GTTTAGCTTAGCGGCCAGCTCATTC-CAGT-3'; S $\gamma$ 1, forward 5'-ATAAGTAGTAGTTGGGGATTC-3' and reverse 5'-CTCAGCCTGGTACCTTATACA-3'. Data were normalized to input chromatin DNA and depicted as enrichment of each amplicon DNA relative to baseline value obtained using an irrelevant mAb.

### *Aicda* and *IgH* locus Germline I $\mu$ -C $\mu$ , circle I $\gamma$ 1- C $\mu$ and Post-recombination I $\mu$ -C $\mu$ Transcripts

RNA was extracted from  $2 \times 10^6$  cells using the RNeasy Mini Kit (Qiagen) according to the manufacturer's protocol. Levels of *Aicda* transcripts, germline I $\mu$ -C $\mu$  and I $\gamma$ 1-C $\gamma$ 1 transcripts, circle I $\gamma$ 1- C $\mu$  transcripts and post-recombination I $\mu$ -C $\gamma$ 1 transcripts were quantified by reverse transcription (RT) and real-time quantitative PCR (qPCR). First-strand cDNAs were synthesized from equal amounts of total RNAs (2  $\mu$ g) using the SuperScript<sup>TM</sup> III First-Strand Synthesis System (Invitrogen). Real-time qPCR

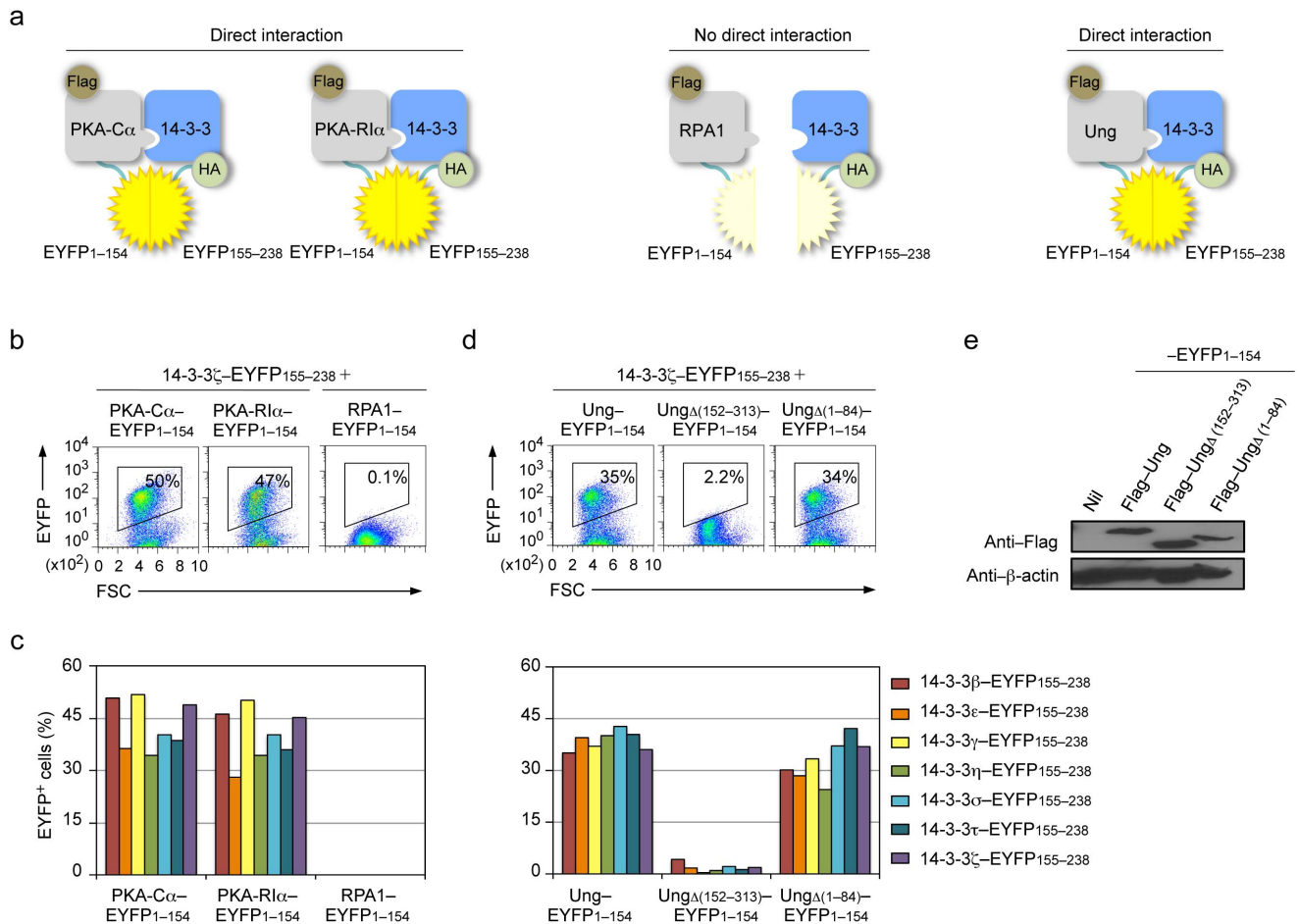


**Figure 2. 14-3-3 adaptors interact with PKA and Ung.** (a) Schematics of the principle of the BiFC assays to analyze interaction of 14-3-3 (HA-14-3-3-EYFP155-238) with PKA-C $\alpha$  (Flag-PKA-C $\alpha$ -EYFP1-154), PKA-Rl $\alpha$  (Flag-PKA-Rl $\alpha$ -EYFP1-154), RPA1 (Flag-RPA1-EYFP1-154) or Ung (Flag-Ung-EYFP1-154). (b) BiFC assays of the interaction between 14-3-3 $\zeta$  (fused to EYFP155-238) and PKA-C $\alpha$  and PKA-Rl $\alpha$ , but not RPA1 (fused to EYFP1-154) in HeLa cells, as analyzed by flow cytometry. (c) Quantification of the interaction between each of the seven 14-3-3 isoforms ( $\beta$ ,  $\epsilon$ ,  $\gamma$ ,  $\eta$ ,  $\sigma$ ,  $\tau$ ,  $\zeta$ ; fused to EYFP155-238) and PKA-C $\alpha$ , and PKA-Rl $\alpha$  or RPA1 (fused to EYFP1-154, left panel), and Ung, and Ung $\Delta$ (152-313) or Ung $\Delta$ (1-84) (fused to EYFP1-154, right panel) in HeLa cells depicted as percentage of EYFP $^{+}$ , as analyzed by flow cytometry. (d) BiFC assays of the interaction between 14-3-3 $\zeta$  (fused to EYFP155-238) and Ung and N-terminal truncation mutant Ung $\Delta$ (1-84), but not C-terminal truncation mutant Ung $\Delta$ (152-313) (fused to EYFP1-154) in HeLa cells, as analyzed by flow cytometry. (e) Immunoblotting using specific mAbs to identify Flag and  $\beta$ -actin in HeLa cell expressing nil (pcDNA3 vector), Flag-Ung, Flag-Ung $\Delta$ (152-313), Flag-Ung $\Delta$ (1-84) (fused to EYFP1-154). Data are representative of those from three independent experiments.

doi:10.1371/journal.pone.0080414.g002

analysis was performed using the DNA Engine Opticon Real-Time PCR Detection System (Bio-Rad Laboratories) to measure SYBR-green (DyNamo HS SYBR Green) incorporation with the following protocol: 50°C for 2 min, 95°C for 10 min, 40 cycles of 95°C for 10 sec, 60°C for 20 sec, 72°C for 30 sec, 80°C for 1 sec, and data acquisition at 80°C, and 72°C for 10 min. Melting curve analysis was performed from 72°C–95°C and samples were incubated for another 5 min at 72°C. The  $\Delta\Delta C_t$  method was used to analyze levels of transcripts and data were normalized to levels of *Gapdh* transcripts. For qPCR, the following primers were used: *Aicda* transcripts, forward 5'-TGCTACGTGGTGAAGAGAGAG-3' and reverse 5'-TCCCAGTCTGAGATGTAGCG-3'; germline I $\mu$ -C $\mu$  transcripts, forward 5'-ACCTGGGAATGTATGGTTGTGGCTT-3' and reverse 5'-TCTGAACCTT-CAAGGATGCTCTTG-3'; germline I $\gamma$ 1-C $\gamma$ 1 transcripts, forward 5'-TCGAGAAGCCTGAGGAATGTG-3' and reverse 5'-ATGGAGTTAGTTTGGCAGCA-3'; circle I $\gamma$ 1-C $\mu$  transcripts, forward 5'-GGCCCTTCCAGATCTTTGAG-3' and

reverse 5'-ACCTGGGAATGTATGGTTGTGGCTT-3'; post-recombined I $\mu$ -C $\gamma$ 1 transcripts, forward 5'-ACCTGGGAATGTATGGTTGTGGCTT-3' and reverse 5'-ATGGAGT-TAGTTTGGCAGCA-3'; *Gapdh* transcripts, forward 5'-TTCACCACCATGGAGAAGGC-3' and reverse 5'-GGCATG-GACTGTGGTCATGA-3'.

#### GST pull-down Assays

Spleen B cells ( $10^7$ ) were stimulated with LPS plus mL-4 for 48 hours. Cells were collected and resuspended in lysis buffer (20 mM of Tris-Cl, pH 7.5, 150 mM of NaCl, 0.5 mM of EDTA, 0.25% (v/v) of NP-40) supplemented with phosphatase inhibitors Na $_4$ P $_2$ O $_7$  (1 mM), NaF (10 mM) and NaVO $_3$  (1 mM) and a cocktail of protease inhibitors (Sigma). After sonication and centrifugation, protein lysates were precleared with immobilized Glutathione Magnetic Beads (Pierce) bound to glutathione S-transferase (GST) for 1 hour at 4°C. Precleared whole cell lysates were then probed with immobilized Glutathione Magnetic Beads

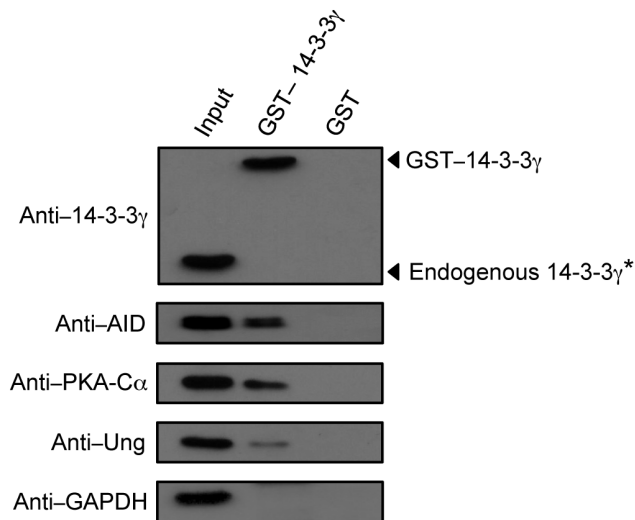


**Figure 3. 14-3-3 $\gamma$  interacts with AID, PKA-C $\alpha$  and Ung expressed in B cells undergoing CSR.** Immunoblotting using specific mAbs/Abs was performed to identify 14-3-3 $\gamma$ , AID, PKA-C $\alpha$  and Ung in proteins pulled-down with GST-14-3-3 $\gamma$  or GST alone from whole lysates of mouse B cells stimulated with LPS plus mL-4 for 48 hours. \*Endogenous 14-3-3 $\gamma$  was detected when a higher amount of GST-14-3-3 $\gamma$ -precipitated proteins were analyzed, but no signal was detected for AID, PKA or Ung from GST-precipitated proteins. Data are representative of those from three independent experiments. doi:10.1371/journal.pone.0080414.g003

bound to either GST or GST-14-3-3 $\gamma$  for 1 hour at 4°C. After three times of washing with lysis buffer, protein complexes were eluted in the SDS sample buffer and fractionated by SDS-PAGE.

### Immunoblotting

Fractionated protein complexes were transferred onto polyvinylidene difluoride (PVDF) membranes (Thermo Scientific) at 4°C. After blocking and overnight incubation with rabbit anti-14-3-3 $\gamma$  Ab (catalog # 18647, IBL, Inc.), mouse anti-AID mAb (catalog # 39-2500, Invitrogen), rabbit anti-PKA $\alpha$  cat Ab (catalog # 903, Santa Cruz Biotechnology), rabbit anti-Ung Ab (catalog # 103236, GeneTex), mouse anti-GAPDH mAb (catalog # 239, GeneTex), mouse anti-Flag mAb (catalog # F3165, Sigma) or mouse anti- $\beta$ -actin mAb (catalog # A5441, Sigma) the membranes were incubated with horseradish peroxidase (HRP)-conjugated secondary Abs. After washing with 0.05% PBS-Tween 20, bound HRP-conjugated Abs were detected using Amersham ECL Plus Western Blotting Detecting Reagents (GE Healthcare).

### Image Analysis

To detect codistributing molecules, human B cells were spun onto cover slips pre-coated with 10  $\mu$ g/ml poly-D-lysine (Sigma-Aldrich), fixed with 2% paraformaldehyde and permeabilized with 0.25% Triton X-100. After blocking with 1% BSA, cells were stained with a rabbit anti-14-3-3 Ab (catalog # ab6081, Abcam) and a mouse anti-AID mAb (catalog # 39-2500, Invitrogen) or a mouse anti-RPA/p34 mAb (catalog # MS-691-P1, NeoMarkers), followed by staining with FITC-conjugated goat anti-rabbit and TRITC-conjugated goat anti-mouse IgG Ab. Confocal microscopy images of spontaneously switching 4B6 B cells cultured at  $5 \times 10^4$  cell/ml in (FBS-RPMI) and human 2E2 B cells stimulated with nil or anti-hCD40 mAb plus hIL-4 were captured by an LSM510-META NLO multi-photon confocal microscope and analyzed using the laser scanning microscope (LSM) Image

Examiner software (Carl Zeiss Microimaging, Inc.). Each pixel in individual cells was analyzed for intensity in green (14-3-3) and red (AID or RPA). The ratio of the number of yellow pixels, to the total number of yellow and green pixels was used to quantify the percentage of 14-3-3 molecules codistributing with AID or RPA.

To detect nuclear foci, spontaneously switching human 4B6 B cells or primary mouse B cells stimulated with LPS plus mL-4 were washed and then extracted in cytoskeletal (CSK) buffer to deplete soluble cytoplasmic and nuclear components before resuspended in 4% paraformaldehyde in PBS to crosslink chromosomal DNA and bound proteins. Cells were then processed, stained and immunofluorescence images were taken at multiple confocal planes. Such  $z$ -stacked images were deconvoluted to generate high-resolution images. All images were pseudo-colored for presentation. B cells were scored as positive for colocalization of 14-3-3 nuclear foci with AID nuclear foci or RPA nuclear foci when showing at least two colocalizing foci, defined as spots within the top 75% pixel intensity of each fluorescence on the pixel intensity map by the Autoquant<sup>®</sup> X software (Media Cybernetics, Inc.). The percentages of positive cells at 0 hour, 24 hours and 48 hours of stimulation were plotted against time points and the Mander's overlapping coefficient were calculated to be between 0.91-0.99 (maximum is 1.0), thereby reflecting a time-dependent increase of colocalization. Processing and staining of mouse primary B cells or human 4B6 B cells were performed following a protocol for foci formation analysis [31].

### Retroviral Transduction

The coding sequence of GFP-Vpr (originally from the pGFP-Vpr plasmid, catalog # 11386, *The NIH AIDS Research and Reference Reagents Program*) was cloned into the retroviral vector pCSretTAC to generate pTAC-GFP-Vpr (generation of pTAC-GFP was described before [23]). Retroviral constructs were transfected along with the pCL-Eco retrovirus-packaging vector into HEK293T cells using the ProFection Mammalian Transfection System<sup>®</sup> (Promega). Transfected cells were cultured in FBS-RPMI in the presence of chloroquine (25  $\mu$ M) for 8 hours. After the removal of chloroquine, retrovirus-containing culture supernatants were harvested every 12 hours for 48 hours. For transduction and CSR analysis, mouse B cells were activated with LPS for 24 hours and then centrifuged at 500  $g$  together with viral particles in the presence of 6  $\mu$ g/ml polybrene (Sigma-Aldrich) for 90 min at 25°C. Transduced B cells were then cultured in virus-free FBS-RPMI in the presence of LPS plus mL-4 for 48 hours for transcript analysis, or for 72 hours for flow cytometry analysis of surface IgG1 and B220 expression in GFP<sup>+</sup> B cells.

### HIV-1 Vpr (15-mer) Peptides

Twenty-two Vpr peptides, each of 15-amino acids in length and each with a sequential 11-amino acid overlap, covering the entire 96-amino acid viral protein, was provided by *The NIH AIDS Research and Reference Reagents Program* (catalog # 6447). Vpr peptides were dissolved in DMSO and then added to LPS-activated B cell cultures for 24 hours, after which B cells were stimulated with LPS plus mL-4 for 72 hours to induce CSR from IgM to IgG1.

### Detection of Vpr in Human B Lymphocytes

Tonsils from HIV-1<sup>-</sup> subjects and lymph nodes from HIV-1<sup>+</sup> patients (UC Irvine Medical Center) were sectioned (7  $\mu$ m) onto glass slides and stained with Abs specific to human using rabbit anti-Vpr Ab (catalog #11836, *NIH AIDS Research and Reference Reagents Program*) alone, or with mouse anti-human CD20 Ab (clone 2H7, eBioscience) or with mouse anti-AID mAb (catalog #

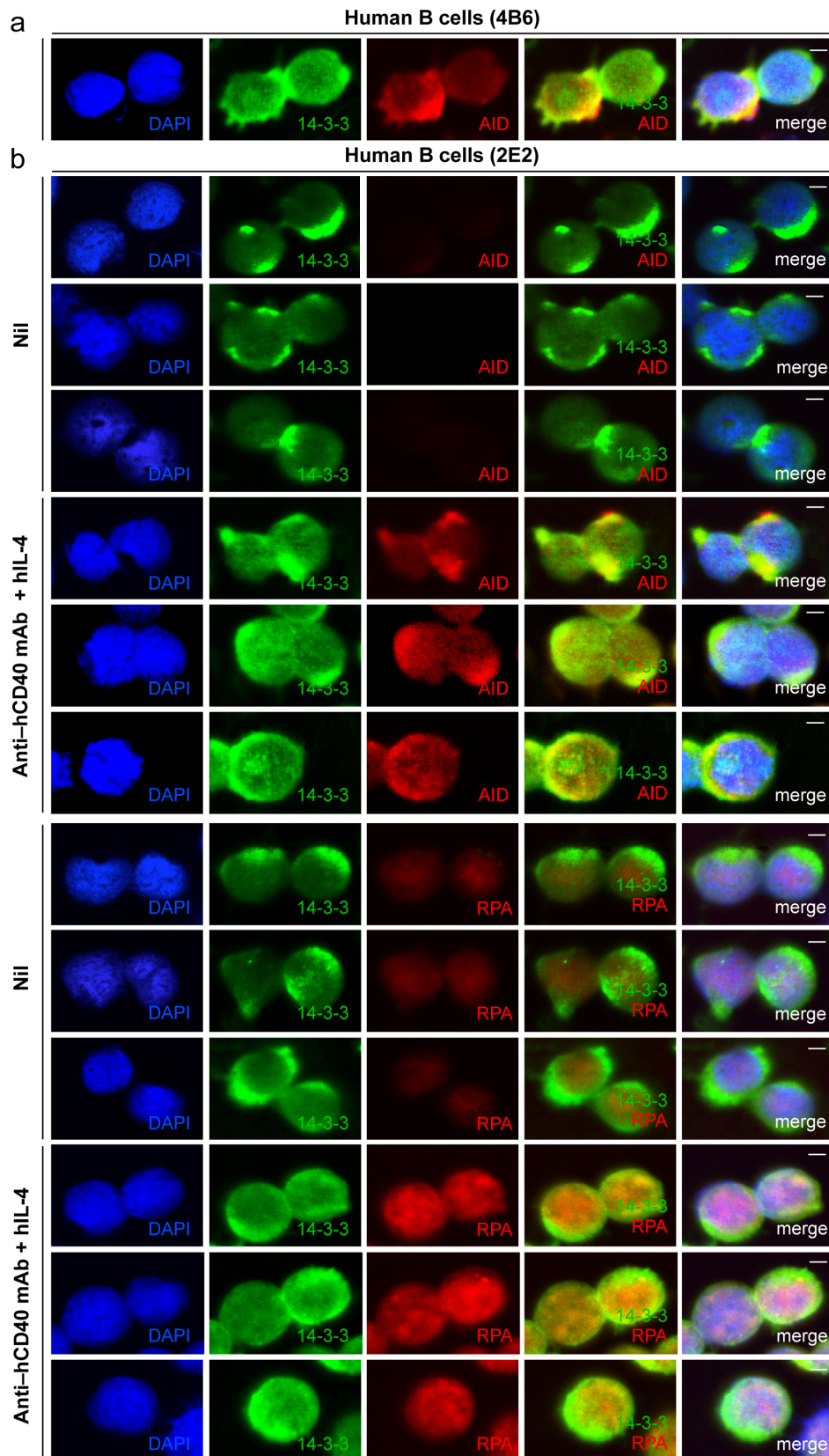


**Figure 4. 14-3-3 adaptors codistribute with AID and RPA in the nucleus of switching B cells.** (a) Codistribution of 14-3-3 and AID in human 4B6 B cells (spontaneous CSR). (b) Codistribution of 14-3-3 with AID or RPA in human 2E2 B cells stimulated with agonistic anti-hCD40 mAb plus hIL-4 (to induce CSR to IgG1) for 48 hours. Scale bars: 5  $\mu$ m. Data are representative of those from three independent experiments. doi:10.1371/journal.pone.0080414.g004

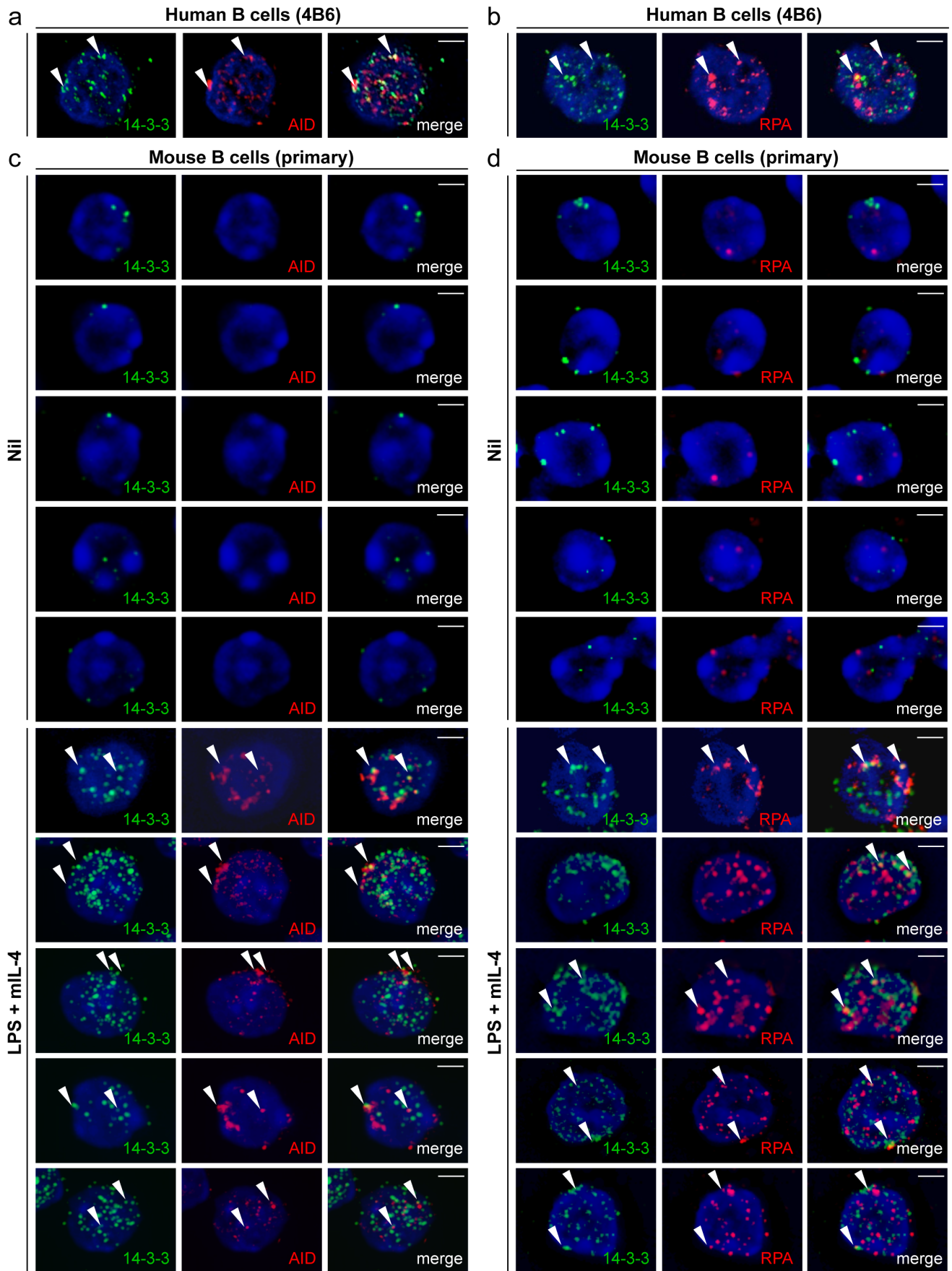


**Figure 5. 14-3-3 adaptors colocalize with AID and RPA in the nucleus of switching B cells.** (a) Formation of 14-3-3 nuclear foci that colocalized with AID nuclear foci in human 4B6 B cells. (b) Formation of 14-3-3 nuclear foci that colocalized with RPA nuclear foci in human 4B6 B cells. (c) Formation of 14-3-3 nuclear foci that colocalized with AID nuclear foci in mouse primary B cells stimulated with LPS plus mL-4 (to induce CSR to IgG1) for 48 hours. (d) Formation of 14-3-3 nuclear foci that colocalized with RPA nuclear foci in mouse primary B cells stimulated with LPS plus mL-4 for 48 hours. Scale bars: 5  $\mu$ m. Data are representative of those from three independent experiments. doi:10.1371/journal.pone.0080414.g005

39–2500, Invitrogen). Color was development by DAB+ chromogen (Dako) and slides were dehydrated and counterstained with hematoxylin. Images were captured at 40X magnification using Nikon Eclipse E400.

To detect B cell uptake of Vpr, human 4B6 B cells were cocultured for 7 days with human CEM.NK<sup>R</sup>-CCR5 T cells infected with nil or HIV-192US657 (a clinical isolate of the primary R5 HIV-1 strain [32–34]), fixed with 2% paraformaldehyde and permeabilized with 0.25% Triton X-100 (Sigma-Aldrich). After blocking with 1% BSA, cells were stained with FITC-conjugated anti- $\mu$  mAb or FITC-conjugated anti-CD4 mAb to identify sIg $\mu$ <sup>+</sup>4B6 cells or CD4<sup>+</sup> CEM.NK<sup>R</sup>-CCR5 T cells, respectively and rabbit anti-Vpr Ab (catalog # 11836, *NIH AIDS Research and Reference Reagents Program*) and Alexa 594-conjugated goat anti-rabbit IgG Ab to identify Vpr uptake for 1 hour. DAPI was used to stain the nucleus. Fluorescence images were captured at 100X magnification. All experiments involving HIV-192US657 were performed in a dedicated Biosafety Level III facility.

### Ethics Statement

Human materials. All human subject materials were surgical remnants collected and maintained for research purposes by the School of Medicine Department of Pathology, University of California, Irvine, CA 92697— under patient privacy rule, no information was disclosed on age, sex and identity of the patient sources of the surgical materials. The use of these materials for research associated with this study was specifically approved by the Institutional Review Board of the University of California, Irvine.

Mice. C57BL/6 mice 8–12 weeks old were housed in a pathogen-free facility and provided with autoclaved food and deionized water. The Institutional Animal Care and Use Committee of the University of California, Irvine, CA 92697, specifically approved the use of mice for the isolation of primary murine B cells for research associated with this study.

### Statistical Analysis

Statistic analysis was performed using Excel<sup>®</sup> software (Microsoft) to determine *P* values by two-tailed paired student's *t*-test. *P* values less than 0.05 were considered significant.

## Results

### 14-3-3 Adaptors Bind AID, but not CSR-defective AID C-terminal Mutants

The direct interaction between 14-3-3 and AID was addressed using BiFC assays. In our BiFC assays, EYFP was split into two complementary moieties: the N-terminal 154 amino acids (EYFP1–154) and the C-terminal 84 amino acids (EYFP155–238) [35,36]. EYFP1–154 was fused with Flag-tagged AID (Flag-AID-EYFP1–154), AID C-terminal truncation mutant (Flag-AID $\Delta$ (180–198)-EYFP1–154), AID C-terminal point mutants (Flag-AIDR190A-EYFP1–154, Flag-AIDF193A-EYFP1–154, Flag-AIDL196A-EYFP1–154) or AID S38A mutant (Flag-AIDS38A-EYFP1–154). EYFP155–238 was fused with influenza hemagglutinin (HA)-tagged 14-3-3 $\beta$ ,  $\epsilon$ ,  $\gamma$ ,  $\eta$ ,  $\sigma$ ,  $\tau$  or  $\zeta$ , (HA-14-3-3 $\beta$ -EYFP155–238, HA-14-3-3 $\epsilon$ -EYFP155–238, HA-14-3-3 $\gamma$ -EYFP155–238, HA-14-3-3 $\eta$ -EYFP155–238, HA-14-3-3 $\sigma$ -EYFP155–238, HA-14-3-3 $\tau$ -EYFP155–238 or HA-14-3-3 $\zeta$ -EYFP155–238, respectively). Upon coexpression of Flag-AID-EYFP1–154 and HA-14-3-3-EYFP155–238 in human HeLa cells, the two EYFP moieties complement each other and give off fluorescence complex (EYFP<sup>+</sup>) only when juxtaposed, as a result of direct interaction between AID and 14-3-3. By contrast, if AID and 14-3-3 interact through a third molecule, this 'spacer' molecule will prevent the direct interaction between AID and 14-3-3, and therefore, hamper EYFP1–154 and EYFP155–238 reciprocal complementation (**Figure 1a**). We have previously shown [23], and confirmed here, that all seven 14-3-3 isoforms interacted with AID and that 14-3-3 $\zeta$  failed to interact with AID $\Delta$ (190–198) or AID $\Delta$ (180–198), which was expressed at a higher level than AID (**Figure 1b, 1c** and not shown), two AID C-terminal truncation mutants that are defective in mediating CSR despite their normal

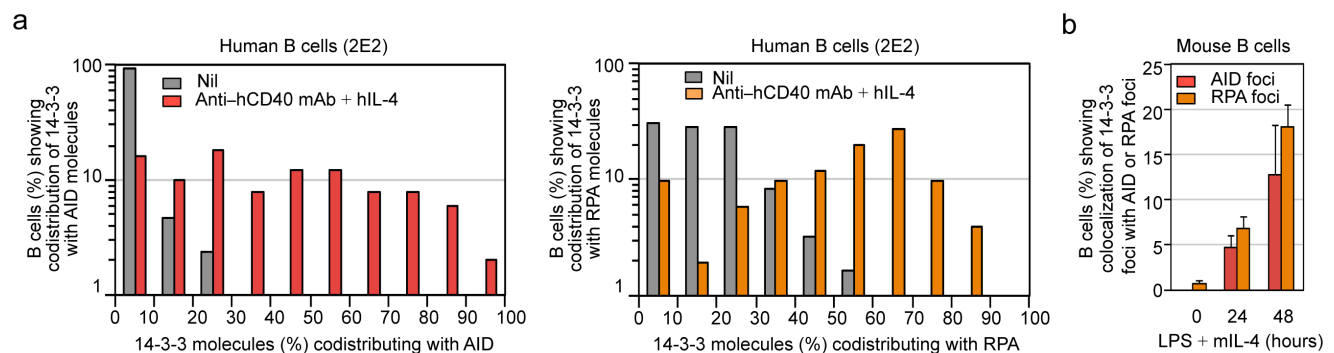


**Figure 6. 14-3-3 adaptors colocalize with AID and RPA at 24 hours and 48 hours.** (a) Percentages of human 2E2 B cells showing 14-3-3 molecules codistributing (%) with AID (red) or RPA (orange) were calculated and depicted on the y-axis. At least 100 cells stimulated with nil or agonistic anti-hCD40 mAb plus hIL-4 were analyzed in each experiment. (b) Quantification of cells showing colocalization of 14-3-3 nuclear foci with AID nuclear foci or RPA nuclear foci in mouse primary B cells stimulated with LPS plus mL-4 for 0 hour, 24 hours and 48 hours (mean and s.e.m. of data from three independent experiments). doi:10.1371/journal.pone.0080414.g006

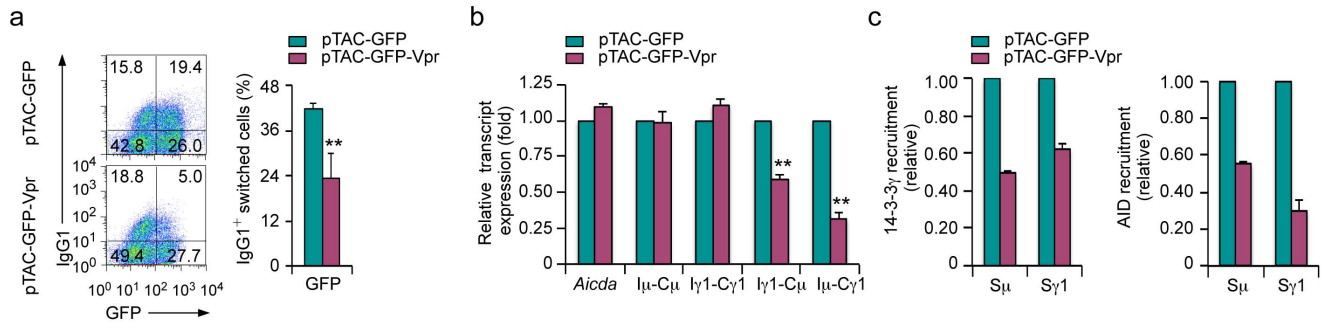


**Figure 7. Inhibition of CSR and disruption of 14-3-3 recruitment to S regions by Vpr.** (a) Proportions of IgG1<sup>+</sup> cells in mouse primary B cells transduced with pTAC-GFP-Vpr or pTAC-GFP retrovirus (which mediated expression of GFP-Vpr or GFP, respectively) and stimulated with LPS plus mL-4 for 72 hours (left; to induce CSR to IgG1), and quantification of class-switched surface IgG1<sup>+</sup> B cells expressing GFP (right; mean and s.e.m of data from three independent experiments), as analyzed by flow cytometry. (b) Levels of *Aicda*, germline Iμ-Cμ and Iγ1-Cγ1, circle Iγ1-Cμ and mature post-recombination Iμ-Cγ1 transcripts in mouse primary B cells expressing GFP-Vpr or GFP and stimulated with LPS plus mL-4 for 48 hours. Data were normalized to the level of *Gapdh* transcripts and depicted as the ratio of expression of transcripts in B cells expressing GFP-Vpr to that in B cells expressing GFP (mean and s.e.m of data from three independent experiments). \*\*,  $P < 0.01$ , t-test. (c) ChIP-qPCR analysis of the binding of 14-3-3γ and AID to the Sμ and Sγ1 region DNA in mouse primary B cells expressing GFP-Vpr or GFP and stimulated with LPS plus mL-4 for 48 hours. Data were normalized to input chromatin DNA and depicted as enrichment of each DNA amplicon relative to baseline value obtained using irrelevant Ab. Data are representative of those from three independent experiments. doi:10.1371/journal.pone.0080414.g007

DNA dC deamination activity [37]. In addition, 14-3-3ζ displayed reduced (by 66%) interaction with AID C-terminal point-mutant AIDF193A (Figure 1c), which fails to mediate CSR, despite its predominant nuclear localization [38,39]. 14-3-3ζ also displayed reduced interaction with another CSR-defective AID C-terminal point-mutant AIDL196A. By contrast, 14-3-3ζ directly interacted with AIDR190A (Figure 1c), which can fully rescue CSR in *Aicda*<sup>-/-</sup> B cells [38]. Like 14-3-3ζ, the other six 14-3-3 isoforms interacted with AIDR190A, but failed to interact with AIDΔ(180–198), AIDF193A or AIDL196A. Finally, all seven 14-3-3 adaptors directly interacted with AIDS38A mutant, which can be recruited to S region DNA [27], but cannot be phosphorylated by PKA and mediates limited CSR [28] (Figure 1d).

Thus, all seven isoforms of 14-3-3 adaptors interact with AID and a CSR-proficient AID C-terminal point-mutant, but not with CSR-defective AID C-terminal truncation mutant or point-mutants.

#### 14-3-3 Adaptors bind PKA and Ung but not RPA

The direct interaction between 14-3-3 and PKA-Cα and PKA-R1α or RPA1 was addressed using BiFC assays. The kinase activity of the two catalytic subunits PKA-Cα and PKA-Cβ within the PKA holoenzyme is inhibited by the two regulatory inhibitory subunits PKA-R1α and PKA-R2α; upon allosteric binding of cAMP, these two regulatory subunits are released – PKA-R1α is the major PKA regulatory subunit and has been shown to interact

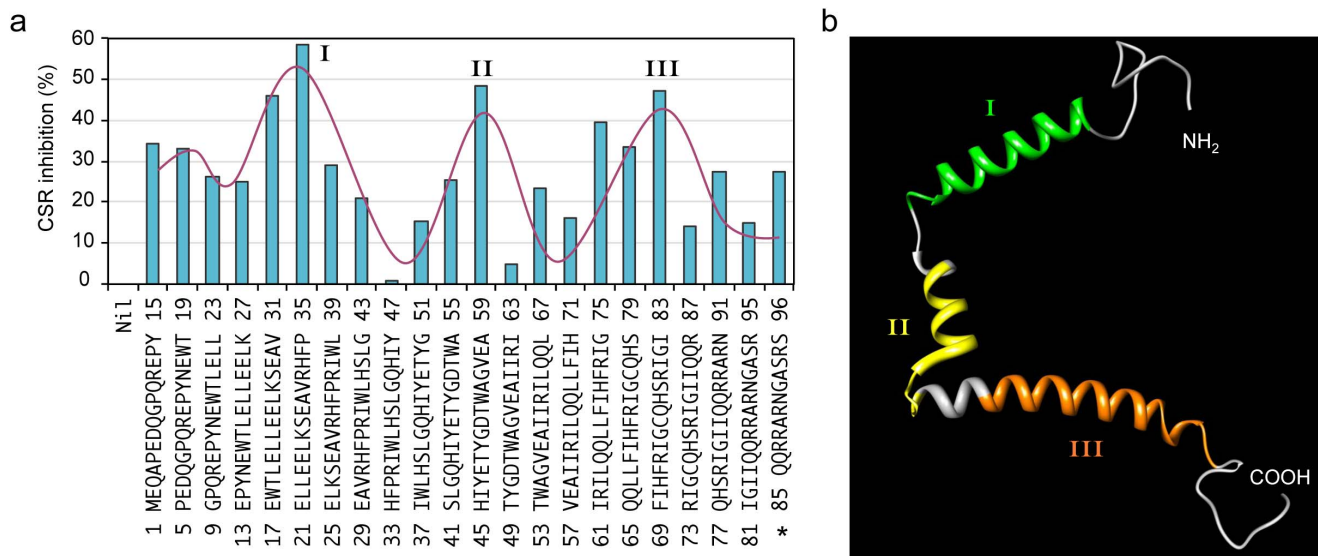


**Figure 8. Vpr peptides inhibit CSR through segregated inhibitory clusters.** (a) Percent of inhibition of CSR to IgG1 in mouse primary B cells stimulated with LPS plus mL-4 in the presence of 22 sequential Vpr peptides (\*denotes the C-terminal peptide, which is 12-amino acid long). Three Vpr peptide clusters with the highest CSR inhibitory effects are depicted as I, II and III. Data are representative of those from three independent experiments. (b) The three Vpr peptide clusters with the highest CSR inhibitory effects correspond to the three α-helices of Vpr. The graph was rendered by the UCSF Chimera® software using the NMR structure of Vpr (PDB ID 1esx). doi:10.1371/journal.pone.0080414.g008

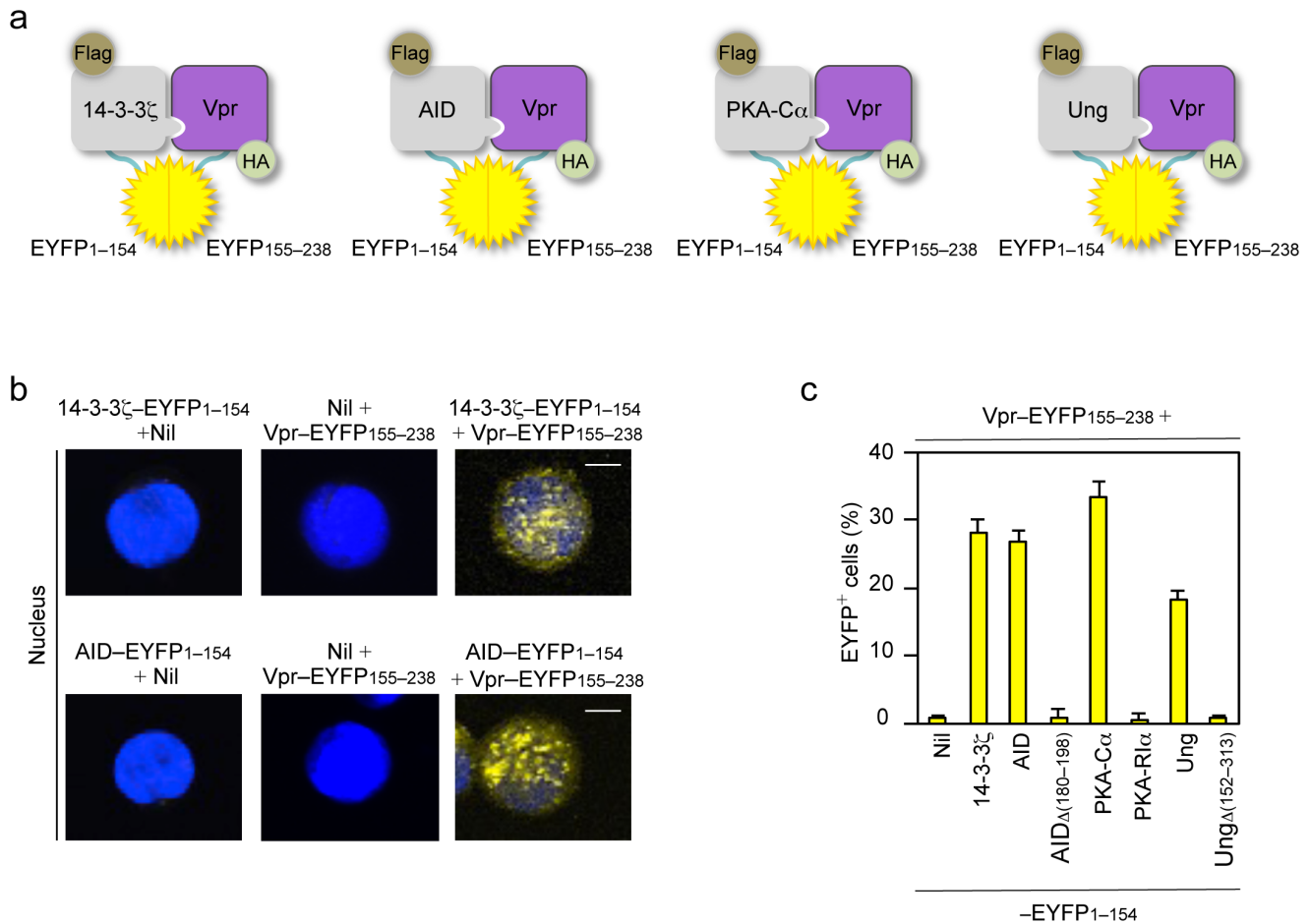


**Figure 9. Essential CSR factors interact with Vpr.** (a) Schematics of the principle of the BiFC assays to analyze interaction of 14-3-3 $\zeta$  (Flag-14-3-3 $\zeta$ -EYFP1-154), AID (Flag-AID-EYFP1-154), PKA-C $\alpha$  (Flag-PKA-C $\alpha$ -EYFP1-154) or Ung (Flag-Ung-EYFP1-154) with Vpr (HA-Vpr-EYFP155-238). (b) BiFC assays of the interaction between 14-3-3 $\zeta$  or AID (fused to EYFP1-154) and Vpr (fused to EYFP155-238) in HeLa cells. DAPI (blue) was used to visualize the nucleus. Scale bars: 5  $\mu$ m. (c) Quantification of the interaction between nil (pcDNA3 vector), 14-3-3 $\zeta$ , AID, AID $\Delta$ (180-198), PKA-C $\alpha$ , PKA-R1 $\alpha$ , Ung or Ung $\Delta$ (152-313) and Vpr in HeLa cells depicted as percentage of EYFP<sup>+</sup>, as analyzed by flow cytometry. Data are representative of those from three independent experiments.  
doi:10.1371/journal.pone.0080414.g009

with AID and be recruited to S region DNA, as part of the PKA holoenzyme [28,40]. In our BiFC assays, HA-tagged 14-3-3 $\beta$ ,  $\epsilon$ ,  $\gamma$ ,  $\eta$ ,  $\sigma$ ,  $\tau$  or  $\zeta$ -EYFP155-238 and Flag-PKA-C $\alpha$ -EYFP1-154, Flag-PKA-R1 $\alpha$ -EYFP1-154 or Flag-RPA1-EYFP1-154 were coexpressed in human HeLa cells. All seven 14-3-3 adaptors directly interacted with PKA-C $\alpha$  and PKA-R1 $\alpha$  (Figure 2a, 2b, 2c). 14-3-3 adaptors, however, did not interact with RPA1 (Figure 2a, 2b, 2c), a 70 kDa subunit that binds single-stranded (ss) DNA [41].

The direct interaction between 14-3-3 and Ung was also addressed using BiFC assays. As we have previously shown, Ung is recruited/stabilized on S region DNA by Rev1, a translesion DNA synthesis (TLS) polymerase, which functions as a scaffold protein in CSR [42], through direct interactions to mediate CSR by processing dUs in S regions for the generation of high density of DSBs. In our BiFC assays, HA-tagged 14-3-3 $\beta$ ,  $\epsilon$ ,  $\gamma$ ,  $\eta$ ,  $\sigma$ ,  $\tau$  or  $\zeta$ -EYFP155-238 and Flag-Ung-EYFP1-154 and Ung N-terminal truncation mutant Flag-Ung $\Delta$ (1-84)-EYFP1-154 and Ung C-terminal truncation mutant Flag-Ung $\Delta$ (152-313)-EYFP1-154 were coexpressed in human HeLa cells. All seven 14-3-3 adaptors directly interacted with Ung and with Ung N-terminal truncation mutant Ung $\Delta$ (1-84), which can rescue CSR in Ung<sup>-/-</sup> B cells

[43,44]. 14-3-3 adaptors, however, did not bind Ung C-terminal truncation mutant Ung $\Delta$ (152-313), which was expressed at a higher level than Ung or Ung $\Delta$ (1-84) (Figure 2c, 2d, 2e).

Thus, all seven isoforms of 14-3-3 adaptors interact with both catalytic and regulatory subunits of PKA and with Ung in a manner dependent on Ung C-terminal amino acid residues, but not with RPA.

#### 14-3-3 $\gamma$ Interacts with AID, PKA-C $\alpha$ and Ung in B Cells Undergoing CSR

To confirm that 14-3-3 $\gamma$  can interact with AID, PKA-C $\alpha$  and Ung in B cells undergoing CSR, we performed glutathione S-transferase (GST) pull-down experiments using 14-3-3 $\gamma$  fused to GST (GST-14-3-3 $\gamma$ ) and whole cell lysates prepared from mouse B cells stimulated with LPS plus mIL-4 for 48 hours. Using immunoblotting, we readily detected AID, PKA-C $\alpha$  and Ung among protein molecules after pull-down by GST-14-3-3 $\gamma$ , but not GST (Figure 3). GST-14-3-3 $\gamma$  was also detected, as expected, and endogenous 14-3-3 $\gamma$  was detectable when a higher amount of GST-14-3-3 $\gamma$ -precipitated proteins were analyzed (data not shown).

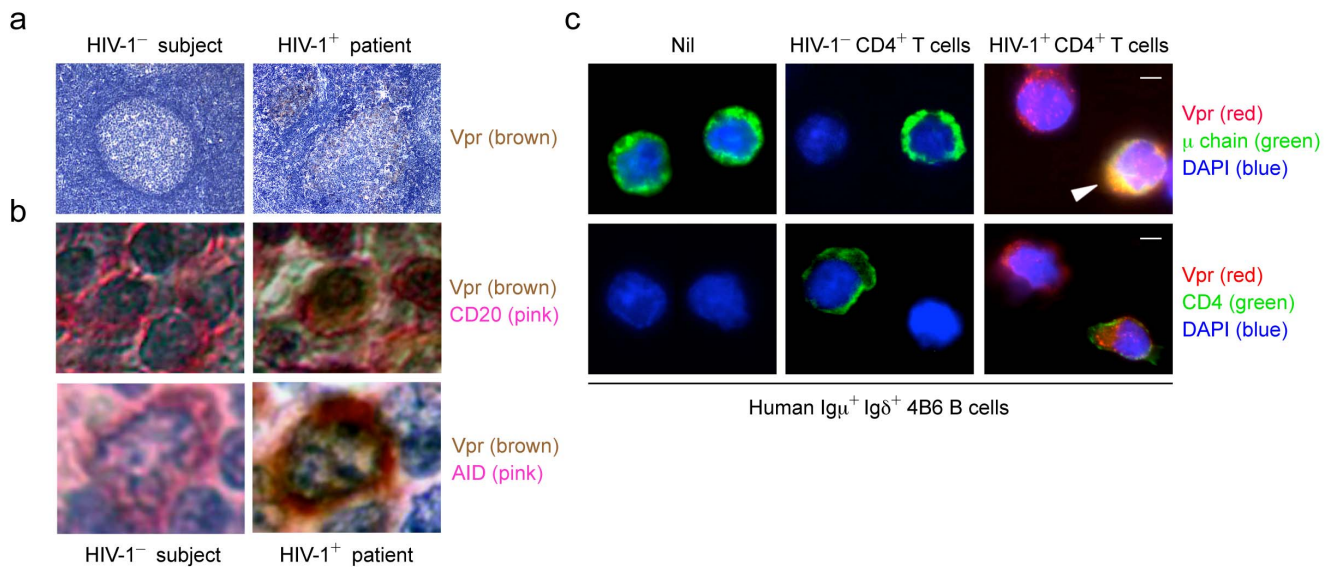


**Figure 10. AID colocalized with Vpr in germinal center B cells from HIV-1<sup>+</sup> patients.** (a) Immunohistochemistry analysis of Vpr in germinal centers in the tonsil from an HIV-1<sup>-</sup> subject (left) or in lymph nodes from an HIV-1<sup>+</sup> patient (right). Original magnification 100 $\times$ . (b) Immunohistochemistry analysis of Vpr and CD20 (top) or Vpr and AID (bottom) in the tonsil from an HIV-1<sup>-</sup> subject (left) or in lymph nodes from an HIV-1<sup>+</sup> patient (right). Original magnification 100 $\times$ . (c) Immunofluorescence staining and confocal microscopy analysis of Vpr in human 4B6 B cells cocultured with nil (left), CEM.NK<sup>R</sup>-CCR5 T cells (middle) or CEM.NK<sup>R</sup>-CCR5 T cells infected with HIV-192US657 (right). Human 4B6 B cells and CEM.NK<sup>R</sup>-CCR5 T cells were stained by FITC-conjugated anti- $\mu$  Ab (top) and anti-CD4 mAb (bottom), respectively. DAPI (blue) was used to visualize the nucleus. Scale bars: 5  $\mu$ m. Data are representative of those from three independent experiments. doi:10.1371/journal.pone.0080414.g010

Thus, 14-3-3 $\gamma$  interacts with AID, PKA-C $\alpha$  and Ung in switching B cells, consistent with its direct interactions with these CSR factors shown by our BiFC assays.

#### 14-3-3 Adaptors Colocalize with AID and RPA in Nuclei of Switching B Cells

As we have shown, 14-3-3 $\zeta$ -AID interaction mainly occurs in the nucleus despite their predominant cytoplasmic localization [23]. Using confocal microscopy we found that, consistent with their direct interaction, 14-3-3 adaptors and AID were expressed and codistributed mainly in the cytoplasm and, to a lower degree, in the nucleus of human 4B6 B cells, which switch spontaneously from IgM to IgG, IgA and IgE [23,45] (Figure 4a). Also, 14-3-3 codistributed with AID and RPA in human 2E2 B cells upon stimulation by an agonistic anti-hCD40 mAb plus hIL-4, which induce human 2E2 B cells to undergo CSR from IgM to IgG and IgE [23] (Figure 4b). To directly visualize the colocalization of 14-3-3 and AID or RPA in the nucleus, where CSR occurs, we adapted a protocol to deplete human and mouse B cells of cytosolic constituents and then identified 14-3-3, AID or RPA by specific Abs. As detected by this approach, 14-3-3, AID and RPA formed nuclear foci in spontaneously switching human 4B6 B cells (Figure 5a, 5b) and in mouse B cells stimulated by LPS plus mL-4 to undergo CSR from IgM to IgG1 at high levels, after 24 and 48 hours (Figure 5c, 5d). We consistently detected two to four 14-3-3-containing nuclear foci that colocalized with AID-containing nuclear foci or RPA-containing nuclear foci (Figure 5), in spite of no direct interaction between 14-3-3 and RPA (Figure 2b). The percentages of human 2E2 B cells showing 14-3-3 molecules codistributing (%) with AID or RPA that were stimulated with agonistic anti-hCD40 mAb plus hIL-4 were higher than those of 2E2 B cells stimulated with nil (Figure 6a). The proportion of B cells that displayed colocalization of 14-3-3 nuclear foci with AID nuclear foci or RPA foci increased over time

of stimulation from 0% to 4.7% within 24 hours, to 12.7% within 48 hours for AID, or from 0.8% to 6.8% within 24 hours, to 18.1% within 48 hours for RPA, consistent with increased proportions of IgG1<sup>+</sup> B cells (typically 5% within 48 hours, 15% within 72 hours and 30% within 96 hours, not shown) under the same stimulation conditions (Figure 6b).

Thus, 14-3-3 adaptors colocalize with AID and RPA in the nucleus of human and mouse B cells undergoing CSR.

#### 14-3-3 and AID Recruitment to S Regions and B Cell CSR are Inhibited by Vpr

Prompted by our findings that 14-3-3 adaptors directly interacted and colocalized with AID and other CSR factors in the nucleus of switching B cells, we hypothesized that 14-3-3-mediated recruitment of the AID-centered CSR machinery to S regions would be blocked when interactions of 14-3-3 with CSR factors were disrupted by naturally occurring or synthetic molecules, leading to CSR inhibition. To test this hypothesis, we first analyzed CSR inhibition by utilizing the HIV-1 accessory protein Vpr, which has been suggested to bind to 14-3-3 proteins [46], Ung [43] and possibly PKA [47]. Primary mouse B cells were transduced with pTAC retrovirus to express green fluorescent protein (GFP) alone (pTAC-GFP) or Vpr linked to GFP (pTAC-GFP-Vpr) and then stimulated with LPS and mL-4 for CSR from IgM to IgG1. CSR was inhibited by Vpr, as shown by reduced proportions of IgG1<sup>+</sup> cells (23%) among B cells expressing GFP-Vpr when compared to their counterparts (42%) expressing GFP (Figure 7).

In addition, levels of circle I $\gamma$ 1-C $\mu$  and post-recombination I $\mu$ -C $\gamma$ 1 transcripts, which are accurate parameters of ongoing and completed CSR, respectively, were reduced in the presence of Vpr. However, levels of AID expression and germline I $\mu$ -C $\mu$  and I $\gamma$ -C $\gamma$ 1 transcription were normal in B cells expressing Vpr (Figure 7b). To further dissect CSR inhibition by Vpr, we used

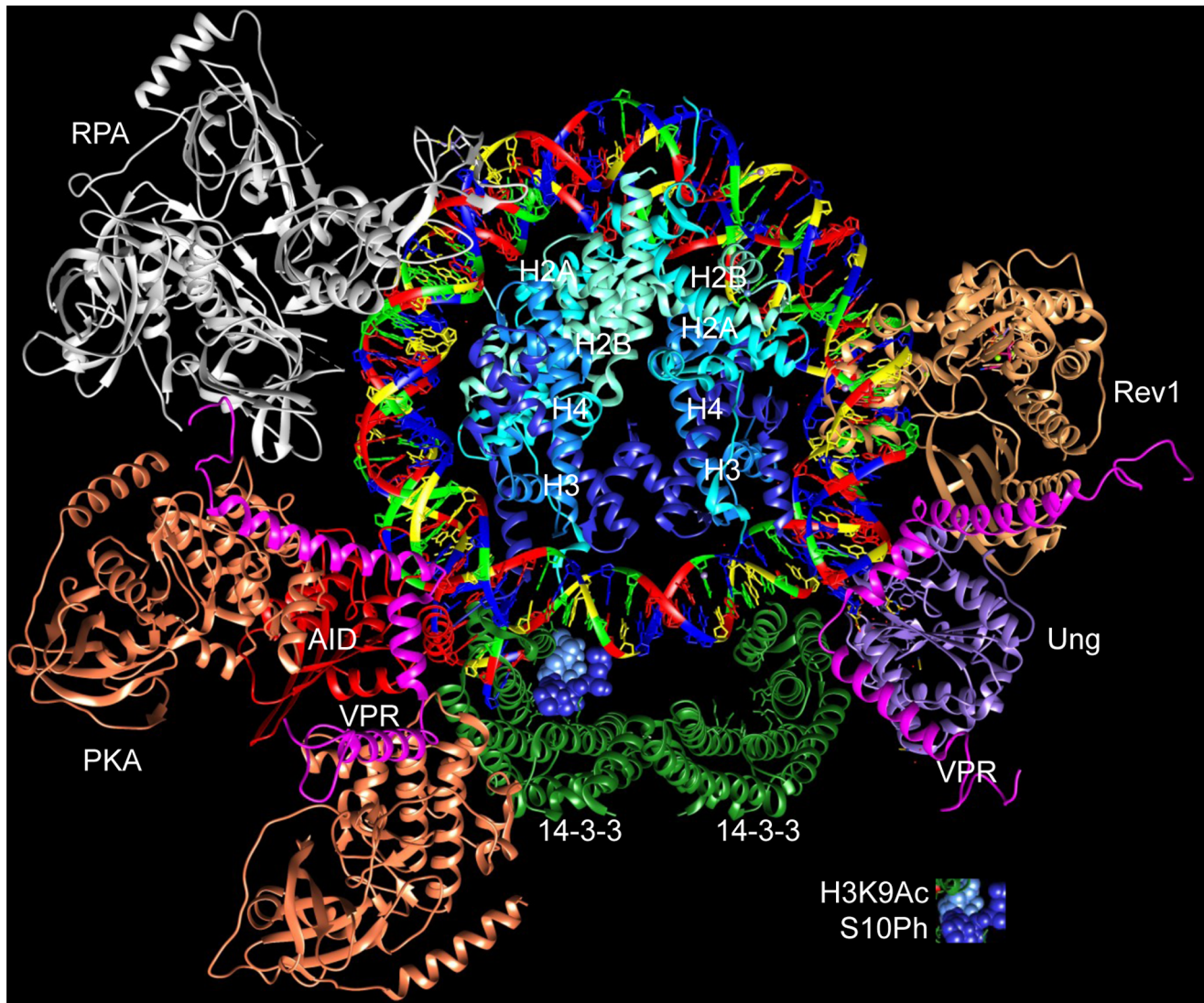


**Figure 11. Schematic illustration of 14-3-3 scaffold functions in the assembly of S region DNA-protein complexes and disruption of such complexes by the naturally occurring Vpr molecule.** A speculative model of a possible configuration of interacting proteins during CSR, and the disruption of some of these complexes by Vpr, as suggested by our current and previous findings [4,23,42]. The CSR macromolecular complex localizes to chromatin S regions through 14-3-3 adaptors (green) binding to the modified histone tail H3K9acS10ph (PDB ID 2c1j) as well as to 5'-AGCT-3' repeats (PDB ID 3afa), which specifically recur in S region DNA. Upon recruitment to S regions by 14-3-3, AID (red, homology modeled after human APOBEC2, PDB ID 2nyt) is phosphorylated at Ser38 by the PKA catalytic subunit (orange, PDB ID 3tnp), leading to the recruitment of RPA (silver, PDB ID 4gop) to S region DNA. Rev1 (brown, PDB ID 3gqc) is important for CSR by virtue of its ability to stabilize Ung (purple, PDB ID 3fci) on S region DNA. Vpr (magenta, PDB ID 1esx) impairs CSR, possibly by disrupting critical DNA-protein interactions, such as S region DNA-14-3-3 binding, and/or protein-protein interactions, such as those between 14-3-3 and AID, PKA or Ung. Graphics were rendered using the UCSF Chimera software (<http://www.cgl.ucsf.edu/chimera>).  
doi:10.1371/journal.pone.0080414.g011

an array of 22 Vpr peptides, each of 15-amino acid in length and each with a sequential 11-amino acid overlap, covering the entire 96-amino acid viral protein. We analyzed CSR inhibition by each peptide in mouse B cells induced by LPS plus mIL-4- uptake of these peptides by B cells was efficient, possibly due to their small size. A differential CSR inhibitory activity was displayed from different Vpr peptides (without affecting B cell proliferation or survival, data not shown), which segregated into three inhibitory clusters (I, II and III) (Figure 8a). The three clusters correlated with the three  $\alpha$ -helices of Vpr [48], which are structurally independent (Figure 8b), and perhaps serve as distinct functional domains for the interaction of the retrovirus with host cell proteins.

To address the molecular mechanisms underlying CSR inhibition by Vpr, we analyzed 14-3-3 $\gamma$  and AID recruitment to S regions in the presence of Vpr. Binding of 14-3-3 $\gamma$  and AID to S $\mu$  and S $\gamma$ 1 DNA was inhibited by Vpr, as shown by our ChIP assays using a specific Ab to 14-3-3 $\gamma$  or AID and chromatin from B cells expressing GFP-Vpr or GFP that were stimulated with LPS plus mIL-4 (Figure 7c). Further, BiFC assays were utilized to address the direct interaction between 14-3-3 or AID and Vpr by coexpressing Flag-14-3-3 $\zeta$ -EYFP1-154 or Flag-AID-EYFP1-154 and HA-Vpr-EYFP155-238, respectively, in HeLa cells. 14-3-3 $\zeta$  and AID indeed interacted with Vpr and they did so in the nucleus (Figure 9a, 9b). Further, in our BiFC assays involving Flag-AID $\Delta$ (180-198)-EYFP1-154, Flag-PKA-C $\alpha$ -EYFP1-154,

Flag-PKA-R1 $\alpha$ -EYFP1-154, Flag-Ung-EYFP1-154 or Flag-Ung $\Delta$ (152-313)-EYFP1-154 with HA-Vpr-EYFP155-238, we showed that PKA-C $\alpha$  and Ung, but not AID $\Delta$ (180-198), PKA-R1 $\alpha$  or Ung $\Delta$ (152-313) interacted with Vpr (**Figure 9c**).

Thus, 14-3-3 adaptors function as scaffolds in mediating the recruitment of AID and possibly PKA and Ung to S regions, which can be inhibited by Vpr, likely due to the disruption of interactions between 14-3-3 and with those CSR factors, leading to the inhibition of CSR.

### AID Colocalize with Vpr in Germinal Center B Cells from HIV-1 Patients

We next addressed the biological relevance of CSR inhibition by Vpr during HIV infection, in which a decrease in class-switched antibodies has been reported to occur [49]. HIV does not infect B cells, but the HIV component such as Nef have been detected in B cells [49]. This prompted us to hypothesize that Vpr is present in secondary lymphoid structures during HIV infection. Here, we analyzed lymph node sections from HIV-1<sup>+</sup> patients and tonsil sections from HIV-1<sup>-</sup> subjects by immunohistochemistry using a specific Ab to Vpr. This revealed Vpr localized within germinal centers of HIV-1<sup>+</sup> patients but not HIV-1<sup>-</sup> subjects (**Figure 10a**). In addition, AID colocalized with Vpr within germinal center B cells of lymph nodes from HIV-1<sup>+</sup> patients but not HIV-1<sup>-</sup> subjects after double staining with an anti-Vpr Ab and anti-AID Ab or anti-CD20 Ab (**Figure 10b**).

To demonstrate that B cells can acquire Vpr from an HIV-1<sup>+</sup> source, we cocultured (HIV-1<sup>-</sup>) human 4B6 B cells with (HIV-1<sup>-</sup>) human CEM.NK<sup>R</sup>-CCR5 T cells infected with nil or HIV-192US657 (a clinical isolate of the primary R5 HIV-1 strain [32-34]). 4B6 B cells displayed Vpr nuclear and cytoplasmic internalization, as indicated by the intracellular staining with FITC-conjugated anti- $\mu$  chain mAb staining and with Alexa 594-conjugated anti-Vpr Ab, only when cocultured with HIV-1-infected T cells, which were specified by staining with FITC-conjugated anti-CD4 mAb and positive for the intracellular staining of Vpr (**Figure 10c**).

Thus, AID colocalizes with Vpr within germinal center B cells of HIV-1<sup>+</sup> patients and can be picked up by HIV-1<sup>-</sup> B cells upon coculturing with HIV-1<sup>+</sup> T cells.

## Discussion

The recruitment and scaffold functions of 14-3-3 adaptors for the stabilization of enzymatic activity of AID and other CSR factors on S regions require multiple molecular interactions. Here, we showed that all seven isoforms of 14-3-3 adaptors directly interacted with AID, but failed to interact with AID C-terminal point mutants that have been shown to be defective in mediating CSR [38,39]. In B cells undergoing CSR, 14-3-3 and AID formed nuclear foci of macromolecular complexes, as suggested by the colocalization of 14-3-3 nuclear foci and AID nuclear foci at 24 hours and 48 hours, but not at 0 hour. Non-colocalizing 14-3-3 nuclear foci may be involved in binding to H3K9acS10ph in the genome (outside the *IgH* locus) for transcription regulation [50]; non-colocalizing AID foci may be responsible for dC deamination outside the *Ig* locus [51-53], particularly in regions where RNA polymerase II stalls [54,55].

All seven isoforms of 14-3-3 adaptors directly interacted with the catalytic and regulatory subunits of the PKA holoenzyme. These would lead to 14-3-3-mediated stabilization of CSR factors on S region DNA and enhancement of AID and PKA activity. 14-3-3 adaptors also directly interacted with Ung, which together with APEs mediates the dominant pathway of DSB generation in

CSR [4,12]. The direct interaction of 14-3-3 adaptors with Ung likely serves two important functions. First, 14-3-3 adaptors possibly facilitate AID and Ung reciprocal stabilization on S region DNA [56], as 14-3-3 possibly bridge AID and Ung to form an AID-14-3-3-Ung complex. This notion is further supported by findings that the reciprocal and cooperative stabilization of AID and Ung depends on the AID C-terminal region, which, as we showed [23], mediates 14-3-3-AID interaction. Second, 14-3-3 may enhance the processing of AID-inserted dUs by Ung for the eventual generation of DSBs. This putative 14-3-3 function would complement and/or enhance that of Rev1, which serves as a scaffold for Ung by stabilizing Ung on S region DNA and enhancing its enzymatic activity [42]. Mismatch repair (MMR) proteins Msh2 and Msh6, recognize deoxyuracil:deoxyguanine mismatches and recruit 5'→3' exonuclease I (ExoI) to the generate DSBs [57], and they stabilize AID on S region DNA in a manner dependent on AID C-terminal region [56]. 14-3-3 adaptors have been shown to interact with ExoI [58,59], suggesting that 14-3-3 adaptors are also involved in MMR-dependent DSB generation. The critical importance of the interaction between 14-3-3 adaptors and essential CSR factors, likely contribute to the assembly of the CSR machinery, which includes AID, Ung, Msh2 and Msh6 [56,57].

14-3-3 nuclear foci colocalized with RPA nuclear foci despite no direct interaction between 14-3-3 and RPA1, the ssDNA-binding subunit, suggesting that RPA1 can only interact with 14-3-3 through another CSR-related factor, such as phosphorylated AID at S38 to form an RPA-AID-14-3-3 complex. RPA has been suggested to mark AID-mediated DNA damage sites [60] and can bind several CSR factors involved in DSB generation, such as Ung [61], MMR elements [62] and the Mre11/Rad50/Nbs1 complex [63]. RPA may also be key to the transition from formation of DSB-generating macromolecular complexes to DSB-resolving complexes on S regions, as RPA can also bind factors that are involved in CSR DSB resolution, such as  $\gamma$ -H2AX, 53BP1 and DNA-PKcs [4].

CSR to IgG1 in primary B cells was significantly reduced in the presence of HIV-1 Vpr; Vpr was also reported to inhibit CSR to IgA in CH12F3 B cells [43]. The CSR inhibitory activities of Vpr segregated within three structural clusters (I, II and III) corresponding to the three Vpr helices, therefore, our studies suggest the notion that CSR inhibition by Vpr is through a “multi-prong” strategy. Interestingly, cluster I peptides encompassed the Ung-binding Vpr region [64] and cluster III peptides straddled the 14-3-3- and PKA-interacting Vpr regions [47,65]. Inhibition of CSR by Vpr did not affect AID expression or germline I<sub>H</sub>-C<sub>H</sub> transcription, suggesting that unlike HIV-1 Nef, which inhibits CSR by interfering with CD40-signaling and NF- $\kappa$ B activation [66], signaling events induced by primary CSR-stimuli and/or secondary CSR-stimuli is not affected by Vpr. By contrast, intimate CSR mechanisms was likely disrupted by Vpr, particularly the binding of 14-3-3 to S region 5'-AGCT-3' repeats, to H3K9acS10ph, or to important CSR factors, such as AID, PKA and Ung. This notion is supported by our data that recruitment of 14-3-3 $\gamma$  to S $\mu$  and S $\gamma$ 1 DNA was disrupted by Vpr, and that essential CSR factors such as 14-3-3 $\zeta$ , AID, PKA-C $\alpha$  and Ung directly interacted with Vpr. Reduced binding of 14-3-3 $\gamma$  to S regions, perhaps in conjunction with putative blocking of 14-3-3 and AID interaction by Vpr, lead to reduced AID recruitment to S $\mu$  and S $\gamma$ 1 DNA. Importantly, proliferation, survival or cell cycle of B cells was not affected in the presence of Vpr, by contrast Vpr-mediated cycle arrest in T cells has been reported [67].

As we have also shown here, AID colocalized with Vpr in HIV-1<sup>+</sup> patients lymph node germinal center B cells. In addition,

HIV-1<sup>-</sup> B cells internalized Vpr when cocultured with HIV-1-infected CD4<sup>+</sup> T cells. B cell internalization of HIV-1 Vpr is likely facilitated by CD21 [68,69], CD40 and/or binding of DC-SIGN [70] – Vpr can be released from virions or infected T cells in an extracellular form in an extracellular form [71], which can be internalized by bystander B cells through protein transduction [72]. Irrespective of Vpr entry route, CSR and the generation of class-switched IgG, possibly including HIV neutralizing IgG antibodies [49,66], is efficiently inhibited by Vpr, leading to HIV-1 evading immune response and persistently infecting the host.

Overall, our findings provide evidence that 14-3-3 adaptor proteins nucleate the assembly of the AID-centered CSR machinery on 5'-AGCT-3' DNA repeats and H3K9acS10ph marks in S regions that are set to undergo S-S recombination (**Figure 11**). They also suggest that CSR DNA-protein and/or protein-protein complexes can be destabilized by naturally occurring molecules, leading to inhibition of CSR, thereby providing a basis for the identification of synthetic small molecule compounds, such as those that disrupt DNA-protein and/or

protein-protein interactions involving 14-3-3 [26,73], or biologics that can effectively inhibit unwanted CSR, such as CSR underlying the generation of IgG and IgA autoantibodies in autoimmunity and atopic IgE antibodies in allergies and asthma.

## Acknowledgments

We are grateful to Dr. Donald Forthal (University of California, Irvine) for HIV-192US657 infected CEM.NK<sup>R</sup>-CCR5 T cells; Dr. Haian Fu (Emory University) for purified recombinant GST-14-3-3 $\gamma$  and GST protein; Dr. Guikai Wu, Dr. Thach Mai, Ariana Longley, Thomas Gocke and Sophia Lam for technical assistance; the UC Irvine Pathology Research Core Facility for immunohistochemistry. NIH AIDS Research and Reference Reagents Program provided Vpr peptides, anti-Vpr Ab and pGFP-Vpr plasmid.

## Author Contributions

Conceived and designed the experiments: ZX PC. Performed the experiments: TL LMT CAW GL EJP ZX. Analyzed the data: TL LMT CAW GL EJP ZX PC. Contributed reagents/materials/analysis tools: TL LMT CAW GL EJP ZX PC. Wrote the paper: TL ZX PC.

## References

1. Stavnezer J, Guikema JE, Schrader CE (2008) Mechanism and regulation of class switch recombination. *Annu Rev Immunol* 26: 261–292.
2. Casali P (2013) Somatic recombination and hypermutation in the immune system. In: Krebs JE, Goldstein ES, Kilpatrick ST, editors. *Lewin's Genes XI*. Sudbury, MA: Jones & Bartlett.
3. Xu Z, Fulop Z, Zhong Y, Evinger AJ III, Zan H, et al. (2005) DNA lesions and repair in immunoglobulin class switch recombination and somatic hypermutation. *Ann N Y Acad Sci* 1050: 146–162.
4. Xu Z, Zan H, Pone EJ, Mai T, Casali P (2012) Immunoglobulin class-switch DNA recombination: induction, targeting and beyond. *Nat Rev Immunol* 12: 517–531.
5. Casali P, Pal Z, Xu Z, Zan H (2006) DNA repair in antibody somatic hypermutation. *Trends Immunol* 27: 313–321.
6. Casali P (2009) Somatic recombination and hypermutation in the immune system. In: Krebs JE, Goldstein ES, Kilpatrick ST, editors. *Lewin's Genes X*. Sudbury, MA: Jones & Bartlett. 570–623.
7. Stavnezer J (2011) Complex regulation and function of activation-induced cytidine deaminase. *Trends Immunol* 32: 194–201.
8. Delker RK, Fugmann SD, Papavasiliou FN (2009) A coming-of-age story: activation-induced cytidine deaminase turns 10. *Nat Immunol* 10: 1147–1153.
9. Zan H, Casali P (2013) Regulation of *Aicda* expression and AID activity. *Autoimmunity* 46: 81–99.
10. Conticello SG, Langlois MA, Neuberger MS (2007) Insights into DNA deaminases. *Nat Struct Mol Biol* 14: 7–9.
11. Fritz EL, Papavasiliou FN (2010) Cytidine deaminases: AIDing DNA demethylation? *Genes Dev* 24: 2107–2114.
12. Masani S, Han L, Yu K (2013) Apurinic/pyrimidic endonuclease 1 is the essential nuclease during immunoglobulin class switch recombination. *Mol Cell Biol* 33: 1468–1473.
13. Han L, Mao W, Yu K (2012) X-ray repair cross-complementing protein 1 (XRCC1) deficiency enhances class switch recombination and is permissive for alternative end joining. *Proc Natl Acad Sci USA*.
14. Kinoshita K, Harigai M, Fagarasan S, Muramatsu M, Honjo T (2001) A hallmark of active class switch recombination: transcripts directed by I promoters on looped-out circular DNAs. *Proc Natl Acad Sci USA* 98: 12620–12623.
15. Pone EJ, Zan H, Zhang J, Al-Qahtani A, Xu Z, et al. (2010) Toll-like receptors and B-cell receptors synergize to induce immunoglobulin class-switch DNA recombination: relevance to microbial antibody responses. *Crit Rev Immunol* 30: 1–29.
16. Pone EJ, Zhang J, Mai T, White CA, Li G, et al. (2012) BCR-signalling synergizes with TLR-signalling for induction of AID and immunoglobulin class-switching through the non-canonical NF- $\kappa$ B pathway. *Nat Commun*: doi: 10.1038/ncomms1769.
17. Li G, White CA, Lam T, Pone EJ, Tran DC, et al. (2013) Combinatorial H3K9acS10ph histone modifications in IgH locus S regions target 14-3-3 adaptors and AID to specify antibody class-switch DNA recombination. *Cell Rep* 5: D.O.I 10.1016/j.cellrep.2013.1009.1031.
18. Li G, Zan H, Xu Z, Casali P (2013) Epigenetics of the antibody response. *Trends Immunol*.
19. Unniraman S, Schatz DG (2006) AID and Igh switch region-Myc chromosomal translocations. *DNA Repair* 5: 1259–1264.
20. Storck S, Aoufouchi S, Weill JC, Reynaud CA (2011) AID and partners: for better and (not) for worse. *Curr Opin Immunol* 23: 337–344.
21. Robbiani DF, Nussenzweig MC (2013) Chromosome translocation, B cell lymphoma, and activation-induced cytidine deaminase. *Annu Rev Pathol* 8: 79–103.
22. Diaz M (2013) The role of activation-induced deaminase in lupus nephritis. *Autoimmunity* 46: 115–120.
23. Xu Z, Fulop Z, Wu G, Pone EJ, Zhang J, et al. (2010) 14-3-3 adaptor proteins recruit AID to 5'-AGCT-3'-rich switch regions for class switch recombination. *Nat Struct Mol Biol* 17: 1124–1135.
24. Han L, Masani S, Yu K (2011) Overlapping activation-induced cytidine deaminase hotspot motifs in Ig class-switch recombination. *Proc Natl Acad Sci USA* 108: 11584–11589.
25. Fu H, Subramanian RR, Masters SC (2000) 14-3-3 proteins: structure, function, and regulation. *Annu Rev Pharmacol Toxicol* 40: 617–647.
26. Zhao J, Meyerkord CL, Du Y, Khuri FR, Fu H (2011) 14-3-3 proteins as potential therapeutic targets. *Semin Cell Dev Biol* 22: 705–712.
27. Cheng HL, Vuong BQ, Basu U, Franklin A, Schwer B, et al. (2009) Integrity of the AID serine-38 phosphorylation site is critical for class switch recombination and somatic hypermutation in mice. *Proc Natl Acad Sci USA* 106: 2717–2722.
28. Vuong BQ, Lee M, Kabir S, Irimia C, Macchiarulo S, et al. (2009) Specific recruitment of protein kinase A to the immunoglobulin locus regulates class-switch recombination. *Nat Immunol* 10: 420–426.
29. Park SR, Zan H, Pal Z, Zhang J, Al-Qahtani A, et al. (2009) HoxC4 binds to the promoter of the cytidine deaminase AID gene to induce AID expression, class-switch DNA recombination and somatic hypermutation. *Nat Immunol* 10: 540–550.
30. Mai T, Zan H, Zhang J, Hawkins JS, Xu Z, et al. (2010) Estrogen receptors bind to and activate the HOXC4/HoxC4 promoter to potentiate HoxC4-mediated activation-induced cytosine deaminase induction, immunoglobulin class switch DNA recombination, and somatic hypermutation. *J Biol Chem* 285: 37797–37810.
31. Wu G, Lin YT, Wei R, Chen Y, Shan Z, et al. (2008) Hicc1, a novel microtubule-associated protein required for maintenance of spindle integrity and chromosomal stability in human cells. *Mol Cell Biol* 28: 3652–3662.
32. Forthal DN, Gilbert PB, Landucci G, Phan T (2007) Recombinant gp120 vaccine-induced antibodies inhibit clinical strains of HIV-1 in the presence of Fc receptor-bearing effector cells and correlate inversely with HIV infection rate. *J Immunol* 178: 6596–6603.
33. Forthal DN, Landucci G, Phan TB, Becerra J (2005) Interactions between natural killer cells and antibody Fc result in enhanced antibody neutralization of human immunodeficiency virus type 1. *J Virol* 79: 2042–2049.
34. Hessel AJ, Hangartner L, Hunter M, Havenith CE, Beurskens FJ, et al. (2007) Fc receptor but not complement binding is important in antibody protection against HIV. *Nature* 449: 101–104.
35. Kerppola TK (2006) Design and implementation of bimolecular fluorescence complementation (BiFC) assays for the visualization of protein interactions in living cells. *Nature protocols* 1: 1278–1286.
36. Hu CD, Kerppola TK (2003) Simultaneous visualization of multiple protein interactions in living cells using multicolor fluorescence complementation analysis. *Nature biotechnology* 21: 539–545.
37. Barreto V, Reina-San-Martin B, Ramiro AR, McBride KM, Nussenzweig MC (2003) C-terminal deletion of AID uncouples class switch recombination from somatic hypermutation and gene conversion. *Mol Cell* 12: 501–508.

38. Geisberger R, Rada C, Neuberger MS (2009) The stability of AID and its function in class-switching are critically sensitive to the identity of its nuclear-export sequence. *Proc Natl Acad Sci USA* 106: 6736–6741.
39. Doi T, Kato L, Ito S, Shinkura R, Wei M, et al. (2009) The C-terminal region of activation-induced cytidine deaminase is responsible for a recombination function other than DNA cleavage in class switch recombination. *Proc Natl Acad Sci USA* 106: 2758–2763.
40. Pasqualucci L, Kitaura Y, Gu H, Dalla-Favera R (2006) PKA-mediated phosphorylation regulates the function of activation-induced deaminase (AID) in B cells. *Proc Natl Acad Sci USA* 103: 395–400.
41. Chaudhuri J, Khuong C, Alt FW (2004) Replication protein A interacts with AID to promote deamination of somatic hypermutation targets. *Nature* 430: 992–998.
42. Zan H, White CA, Thomas LM, Mai T, Li G, et al. (2012) Rev1 recruits Ung to switch regions and enhances dU glycosylation for immunoglobulin class switch DNA recombination. *Cell Rep* 2: 1220–1232.
43. Begum NA, Izumi N, Nishikori M, Nagaoka H, Shinkura R, et al. (2007) Requirement of non-canonical activity of uracil DNA glycosylase for class switch recombination. *J Biol Chem* 282: 731–742.
44. Begum NA, Stanlie A, Doi T, Sasaki Y, Jin HW, et al. (2009) Further evidence for involvement of a noncanonical function of uracil DNA glycosylase in class switch recombination. *Proc Natl Acad Sci USA* 106: 2752–2757.
45. Kim EC, Edmonston CR, Wu X, Schaffer A, Casali P (2004) The HoxC4 homeodomain protein mediates activation of the immunoglobulin heavy chain 3' hsl<sub>2</sub> enhancer in human B cells. Relevance to class switch DNA recombination. *J Biol Chem* 279: 42258–42269.
46. Kino T, De Martino MU, Charmandari E, Ichijo T, Outas T, et al. (2005) HIV-1 accessory protein Vpr inhibits the effect of insulin on the Foxo subfamily of forkhead transcription factors by interfering with their binding to 14–3-3 proteins: potential clinical implications regarding the insulin resistance of HIV-1-infected patients. *Diabetes* 54: 23–31.
47. Barnitz RA, Wan F, Tripuraneni V, Bolton DL, Lenardo MJ (2010) Protein kinase A phosphorylation activates Vpr-induced cell cycle arrest during human immunodeficiency virus type 1 infection. *J Virol* 84: 6410–6424.
48. Wecker K, Morellet N, Bouaziz S, Roques BP (2002) NMR structure of the HIV-1 regulatory protein Vpr in H<sub>2</sub>O/trifluoroethanol. *Eur J Biochem* 269: 3779–3788.
49. Xu W, Santini PA, Sullivan JS, He B, Shan M, et al. (2009) HIV-1 evades virus-specific IgG2 and IgA responses by targeting systemic and intestinal B cells via long-range intercellular conduits. *Nat Immunol* 10: 1008–1017.
50. Kellner WA, Ramos E, Van Bortle K, Takenaka N, Corces VG (2012) Genome-wide phosphoacetylation of histone H3 at Drosophila enhancers and promoters. *Genome Res* 22: 1081–1088.
51. Liu M, Duke JL, Richter DJ, Vinaes CG, Goodnow CC, et al. (2008) Two levels of protection for the B cell genome during somatic hypermutation. *Nature* 451: 841–845.
52. Yamane A, Resch W, Kuo N, Kuchen S, Li Z, et al. (2011) Deep-sequencing identification of the genomic targets of the cytidine deaminase AID and its cofactor RPA in B lymphocytes. *Nat Immunol* 12: 62–69.
53. Staszewski O, Baker RE, Ucher AJ, Martier R, Stavnezzer J, et al. (2011) Activation-induced cytidine deaminase induces reproducible DNA breaks at many non-Ig loci in activated B cells. *Mol Cell* 41: 232–242.
54. Pavri R, Gazumyan A, Jankovic M, Di Virgilio M, Klein I, et al. (2010) Activation-induced cytidine deaminase targets DNA at sites of RNA polymerase II stalling by interaction with Spt5. *Cell* 143: 122–133.
55. Kenter AL (2012) AID targeting is dependent on RNA polymerase II pausing. *Semin Immunol* 24: 281–286.
56. Ranjit S, Khair L, Linehan EK, Ucher AJ, Chakrabarti M, et al. (2011) AID binds cooperatively with UNG and Msh2-Msh6 to Ig switch regions dependent upon the AID C terminus. *J Immunol* 187: 2464–2475.
57. Rada C, Di Noia JM, Neuberger MS (2004) Mismatch recognition and uracil excision provide complementary paths to both Ig switching and the A/T-focused phase of somatic mutation. *Mol Cell* 16: 163–171.
58. Andersen SD, Keijzers G, Rampakakis E, Engels K, Luhn P, et al. (2012) 14–3-3 checkpoint regulatory proteins interact specifically with DNA repair protein human exonuclease 1 (hEXO1) via a semi-conserved motif. *DNA Repair* 11: 267–277.
59. Engels K, Giannattasio M, Muzi-Falconi M, Lopes M, Ferrari S (2011) 14–3-3 Proteins regulate exonuclease 1-dependent processing of stalled replication forks. *PLoS Genet* 7: e1001367.
60. Yamane A, Robbiani DF, Resch W, Bothmer A, Nakahashi H, et al. (2013) RPA accumulation during class switch recombination represents 5'-3' DNA-end resection during the S-G<sub>2</sub>/M phase of the cell cycle. *Cell Rep* 3: 138–147.
61. Otterlei M, Warbrick E, Nagelhus TA, Haug T, Slupphaug G, et al. (1999) Post-replicative base excision repair in replication foci. *EMBO J* 18: 3834–3844.
62. Guo S, Zhang Y, Yuan F, Gao Y, Gu L, et al. (2006) Regulation of replication protein A functions in DNA mismatch repair by phosphorylation. *J Biol Chem* 281: 21607–21616.
63. Oakley GG, Tillison K, Opiyo SA, Glanzer JG, Horn JM, et al. (2009) Physical interaction between replication protein A (RPA) and MRN: involvement of RPA2 phosphorylation and the N-terminus of RPA1. *Biochemistry* 48: 7473–7481.
64. Selig L, Benichou S, Rogel ME, Wu LI, Vodicka MA, et al. (1997) Uracil DNA glycosylase specifically interacts with Vpr of both human immunodeficiency virus type 1 and simian immunodeficiency virus of sooty mangabeys, but binding does not correlate with cell cycle arrest. *J Virol* 71: 4842–4826.
65. Kino T, Gragerov A, Valentin A, Tsopanomalou M, Ilyina-Gragerova G, et al. (2005) Vpr protein of human immunodeficiency virus type 1 binds to 14–3-3 proteins and facilitates complex formation with Cdc25C: implications for cell cycle arrest. *J Virol* 79: 2780–2787.
66. Qiao X, He B, Chiu A, Knowles DM, Chadburn A, et al. (2006) Human immunodeficiency virus 1 Nef suppresses CD40-dependent immunoglobulin class switching in bystander B cells. *Nat Immunol* 7: 302–310.
67. Bolton DL, Barnitz RA, Sakai K, Lenardo MJ (2008) 14–3-3 theta binding to cell cycle regulatory factors is enhanced by HIV-1 Vpr. *Biol Direct* 3: 17.
68. Moir S, Malaspina A, Li Y, Chun TW, Lowe T, et al. (2000) B cells of HIV-1-infected patients bind virions through CD21-complement interactions and transmit infectious virus to activated T cells. *J Exp Med* 192: 637–646.
69. Stoiber H, Speth C, Dierich MP (2003) Role of complement in the control of HIV dynamics and pathogenesis. *Vaccine* 21 Suppl 2: S77–82.
70. He B, Qiao X, Klasse PJ, Chiu A, Chadburn A, et al. (2006) HIV-1 envelope triggers polyclonal Ig class switch recombination through a CD40-independent mechanism involving BAFF and C-type lectin receptors. *J Immunol* 176: 3931–3941.
71. Tungathurthi PK, Sawaya BE, Singh SP, Tomkowicz B, Ayyavoo V, et al. (2003) Role of HIV-1 Vpr in AIDS pathogenesis: relevance and implications of intravirion, intracellular and free Vpr. *Biomed Pharmacother* 57: 20–24.
72. Sherman MP, Schubert U, Williams SA, de Noronha CM, Kreisberg JF, et al. (2002) HIV-1 Vpr displays natural protein-transducing properties: implications for viral pathogenesis. *Virology* 302: 95–105.
73. Zhao J, Du Y, Horton JR, Upadhyay AK, Lou B, et al. (2011) Discovery and structural characterization of a small molecule 14–3-3 protein-protein interaction inhibitor. *Proc Natl Acad Sci USA* 108: 16212–16216.